ADP Ribosylation Factor 6 (ARF6) Promotes Acrosomal Exocytosis by Modulating Lipid Turnover and Rab3A Activation*[S]

Leonardo E. Pelletán[‡1], Laila Suhaiman[‡1], Cintia C. Vaquer[‡1], Matías A. Bustos[‡1], Gerardo A. De Blas[‡],
Nicolas Vitale[§2], Luis S. Mayorga[‡], and Silvia A. Belmonte[‡3]

From the [‡]Instituto de Histología y Embriología, CONICET, Facultad de Ciencias Médicas, CC56, Universidad Nacional de Cuyo,
5500 Mendoza, Argentina and the [§]Département Neurotransmission et Sécrétion Neuroendocrine, Institut des Neurosciences
Cellulaires et Intégratives (UPR 3212), CNRS et Université de Strasbourg, 5 Rue Blaise Pascal, 67084 Strasbourg, France

Background: Sperm acrosomal exocytosis requires GTPases, SNAREs, and a complex lipid signaling.
Results: Exocytic stimuli promote ARF6 activation, which accomplishes exocytosis by stimulating PLC and Rab3A.
Conclusion: ARF6 induces acrosome calcium efflux and assembles the fusion machinery leading to membrane fusion.
Significance: This study explores a novel molecular link between ARF6, PLC, and Rab3A and provides insight into the molecular mechanisms of exocytosis and reproduction.

Regulated secretion is a central issue for the specific function of many cells; for instance, mammalian sperm acrosomal exocytosis is essential for egg fertilization. ARF6 (ADP-ribosylation factor 6) is a small GTPase implicated in exocytosis, but its downstream effectors remain elusive in this process. We combined biochemical, functional, and microscopy-based methods to show that ARF6 is present in human sperm, localizes to the acrosomal region, and is required for calcium and diacylglycerol-induced exocytosis. Results from pulldown assays show that ARF6 exchanges GDP for GTP in sperm challenged with different exocytic stimuli. Myristoylated and guanosine 5′-3-O-(thio)triphosphate (GTPγS)-loaded ARF6 (active form) added to permeabilized sperm induces acrosome exocytosis even in the absence of extracellular calcium. We explore the ARF6 signaling cascade that promotes secretion. We demonstrate that ARF6 stimulates a sperm phospholipase D activity to produce phosphatidic acid and boosts the synthesis of phosphatidylinositol 4,5-bisphosphate. We present direct evidence showing that active ARF6 increases phospholipase C activity, causing phosphatidylinositol 4,5-bisphosphate hydrolysis and inositol 1,4,5-trisphosphate-dependent intra-acrosomal calcium release. We show that active ARF6 increases the exchange of GDP for GTP on Rab3A, a prerequisite for secretion. We propose that exocytic stimuli activate ARF6, which is required for acrosomal calcium efflux and the assembly of the membrane fusion machinery. This report highlights the physiological importance of ARF6 as a key factor for human sperm exocytosis and fertilization.

The ADP-ribosylation factors (ARFs)[4] are a family of monomeric GTP-binding proteins belonging to the small GTPases of the Ras superfamily (1). ARFs are grouped into three different classes in mammalian cells based on their size and sequence homology. Class I contains ARF1–3; class II contains ARF4 and ARF5; and class III contains ARF6. ARFs appear to control a variety of vesicle transport and fusion steps in the endocytic and secretory pathways (2).

Like all small G-proteins, ARFs function as molecular switches that alternate between a GTP and membrane-bound "on" state and a GDP-bound, mostly cytosolic, "off" state. During the activation phase of the ARF cycle, a guanine nucleotide exchange factor (GEF) releases GDP bound in the nucleotide pocket. ARF immediately binds GTP, which has a much higher cytosolic concentration than GDP. This is the rate-limiting step in ARF activation. During the inactivation phase, hydrolysis converts GTP to GDP, a reaction catalyzed by ARF's intrinsic GTPase activity assisted by GTPase-activating proteins (GAPs). ARF6 regulates several membrane trafficking pathways, including endosome fusion (3), the modulation of actin assembly, and rearrangement at membranes (4), vesicle biogenesis (5), and also the secretion of preformed vesicles (6).

[4] The abbreviations used are: ARF, ADP-ribosylation factor; 2-APB, 2-aminoethoxydiphenyl borate; AR, acrosome reaction; ARF, ADP-ribosylation factor; DAG, diacylglycerol; GAP, GTPase-activating proteins; GEF, GDP/GTP exchange factor; HTF, human tubal fluid medium; IP$_3$, inositol 1,4,5-trisphosphate; PA, phosphatidic acid; PI4P-5K, phosphatidylinositol 4-phosphate 5-kinase; PIP$_2$, phosphatidylinositol 4,5-bisphosphate; PLC, phospholipase C; PLD1, phospholipase D1; PMA, phorbol 12-myristate 13-acetate; PSA, *Pisum sativum* agglutinin; SLO, streptolysin O; GTPγS, guanosine 5′-3-O-(thio)triphosphate; PABD, phosphatidic acid binding domain; Tricine, N-[2-hydroxy-1,1-bis(hydroxymethyl)ethyl]glycine; GDPβS, guanyl 5′-yl thiophosphate; TeTx, tetanus toxin; MT-2. metallothionein-2 BoNT/C, botulinum neurotoxin C; BoNT/E botulinum neurotoxin E; PVP, poly(vinylpyrrolidinone).

ARF6 Promotes Calcium-regulated Exocytosis

Regulated secretion is a sophisticated biological process that involves mechanisms elicited by intracellular calcium fluctuations in response to extracellular signals. Exocytosis requires the attachment of secretory granules to the plasma membrane and the opening of fusion pores connecting the interior of the granule to the extracellular medium (7). More than a decade ago, the role of ARF6 as a GTPase that plays a fundamental role in vesicle secretion was identified. For instance, ARF6 peptides were shown to inhibit the regulated secretion of constituents of large dense core granules in neuroendocrine cells (8, 9). Expression of inactive ARF6 mutants (10) and ARF6 silencing (11) validated these observations. Furthermore, the expression of a dominant-negative version of an exchange factor for ARF6 inhibited secretion (12). Similar observations were found in various secreting cell types, including rat brain cortex nerve endings (13). At the same time, an important role for specific lipids, including phosphatidic acid (PA) and phosphatidylinositol 4,5-bisphosphate (PIP_2) in membrane fusion was proposed (11, 14), but regulation of their biosynthesis remained poorly understood. Interestingly, ARF6 was shown *in vitro* to directly activate phosphatidylinositol 4-phosphate 5-kinase (PI4P-5K) (15) and phospholipase D (PLD) (16) to generate PIP_2 and PA, respectively. A link between ARF6, PI4P-5K, and PLD has consequently been reported in various secretory cell types (17).

The acrosome is a large and electron-dense membrane-limited granule that overlies the nucleus of the mature spermatozoon. In response to physiological or pharmacological stimuli, sperm undergo exocytosis of this granule in a synchronized wave, with no recycling of components. This is a special type of calcium-dependent exocytosis termed the acrosome reaction (AR) that is a prerequisite for fertilization (18). The AR is an event induced physiologically by the activation of sperm receptors by progesterone or ZP3 (a glycoprotein of the oocyte's zona pellucida). This interaction initiates a complex transduction mechanism leading to multiple fusion points between the outer acrosomal and the overlying plasma membranes, resulting in the release of the acrosomal contents and the exposure of the molecules present on the inner acrosomal membrane.

A common and fundamental feature of physiological and pharmacological acrosomal exocytosis inducers is that they provoke an increase in intracellular multicomponent calcium rises. It is known that a sustained calcium increase through store-operated calcium channels drives exocytosis (19, 20). During exocytosis, there are some parallel and concomitant steps necessary to achieve AR that occurs thereafter. This signaling cascade involves preparation of the fusion machinery that includes SNAREs (21, 22), α-SNAP/NSF (23), synaptotagmin (24), Rab3A (25, 26), and exchange protein directly activated by cAMP (Epac), a GEF protein that links cAMP and intracellular calcium signaling (27, 28). It has been proposed that a soluble adenylyl cyclase is activated by a sustained increase in intracellular calcium, resulting in a cAMP increase that activates Epac. The signaling cascade branches in at least two arms that come back together at the end of the cascade. One branch prepares the SNARE fusion machinery and involves Rab3A activation, and the other activates PLC-ϵ via Rap stimulation, to produce IP_3 and release intracellular calcium from internal stores, the final trigger for membrane fusion.

A drawback for experiments with spermatozoa is the limited, almost null, transcriptional and translational activity of these cells. Controlled plasma membrane permeabilization has been used to gain access to the membrane fusion machinery required for exocytosis in several secretory cells (29, 30). We used a well established streptolysin O (SLO) permeabilization protocol for studying acrosomal granule exocytosis (31–34) that allows the incorporation of exogenous proteins, lipids, and ions into the cytosol. The extracellular calcium acts as an exocytosis inducer mimicking the opening of store-operated calcium channels. Recently, we reported that diacylglycerol (DAG) stimulates acrosomal exocytosis by feeding into a PKC- and PLD1-dependent positive loop that continuously supplies PIP_2 (33). Given that PIP_2, PLD, and its hydrolysis product, PA, have an essential role in calcium- and DAG-induced acrosomal exocytosis, we wondered whether ARF6 was present in sperm to regulate these lipids concentrations and, consequently, exocytosis. Mammalian spermatozoa are a particularly well suited model to study molecular interactions during secretion (35). From the point of view of intracellular trafficking, sperm are specialized for a single membrane fusion event, the exocytosis of the acrosomal granule. This feature is particularly useful to study the role of a multitasking protein like the small GTPase ARF6. In this study, we combine biochemical with functionally based and microscopy-based methods to show that ARF6 is present in human sperm and is required for calcium- and DAG-induced exocytosis. We present evidence that ARF6 promotes the activity of PLD, PI4P-5K, PLC, and an exchange factor for Rab3A during the course of human sperm AR. We propose that exocytotic stimuli activate ARF6, which is capable of inducing acrosomal calcium efflux and promoting the assembly of the fusion machinery, and both pathways are required for achieving membrane fusion. Notably, we identify ARF6 as a key molecule in the regulation of acrosomal exocytosis signaling in human sperm and consequently for fertilization.

EXPERIMENTAL PROCEDURES

Materials—SLO was obtained from Dr. Bhakdi (University of Mainz, Mainz, Germany). Chelerythrine, U73122, U73343, Ro-31-7549, adenophostin A, 2-aminoethoxydiphenylborate (2-APB), xestospongin C, isopropyl β-D-1-thiogalactopyranoside, glutathione, FITC-conjugated *Pisum sativum* agglutinin (FITC-PSA), and EGTA were from Merck; glutathione-Sepharose 4B was from GE Healthcare. Phorbol 12-myristate 13-acetate (PMA), 1,2-dioctanoyl-*sn*-glycerol (DAG) (catalogue number D5156), phosphatidic acid (PA), FIPI hydrochloride hydrate, 1,2-bis(2-aminophenoxy)ethane-*N,N,N′,N′*-tetraacetic acid tetrakis (acetoxymethyl ester) (BAPTA-AM), and A23187 were from Sigma; phosphatidylinositol 4,5-bisphosphate (PIP_2) and phosphatidylinositol 4-phosphate (PI4P) were from Avanti Polar Lipids, Inc. (Alabaster, AL); EGTA-AM and Fluo3-AM were from Invitrogen; [γ-^{32}P]ATP and Chemiluminescence Reagent Plus were from PerkinElmer Life Sciences and Migliore Laclaustra SRL (Buenos Aires, Argentina); 1-butanol was from BDH Chemicals; anti-Rab3A was from Synaptic Systems (mouse monoclonal antibody, purified IgG clone 42.2); anti-

ARF6 (mouse monoclonal anti-human ARF6, ab19871 or ab131261) and anti-PLD1 (rabbit polyclonal anti-human PLD1, ab10585) were from Abcam (Cambridge, UK); anti-SNAP25 (monoclonal mouse antibody, clone 71.1; conserved epitope), anti-RIM, and anti-complexin I/II were from Synaptic Systems; Cy-3-conjugated anti-rabbit and HRP goat-conjugated anti-mouse were from Jackson ImmunoResearch. The rabbit polyclonal anti-GST antibody (purified IgG) was purchased from Chemicon. CAY10593 (N-[2-[4-(5-chloro-2,3-dihydro-2-oxo-$1H$-benzimidazol-1-yl)-1-piperidinyl]-1-methylethyl]-2-naphthalenecarboxamide) was from Cayman Chemical.

The pGEX-4T-1-PABD plasmid was described in Kassas *et al.* (36) and the pGEX4-T1-MT-2 in Begle *et al.* (11). The plasmid pGEX-hPIPKIγ-5 was provided by Dr. Shuzo Sugita (37) (University of Toronto, Canada), pGEX-5X-1-VHS-GAT (from GGA3) by Dr. Julie G. Donalson (Laboratory of Cell Biology, NHLBI, National Institutes of Health, Bethesda), and pGEX-munc13–1 C1 domain by Dr. José Rizo (University of Texas Southwestern Medical Center, Dallas, TX).

Purified Rab3A, botulinum neurotoxin C and E (BoNT/C and BoNT/E), tetanus toxin (TeTx), C2B domain of synaptotagmin VI, and GST-RIM-RBD were produced by M. Bustos (IHEM-CONICET, Universidad Nacional de Cuyo, Mendoza, Argentina) as described previously (38, 39). The plasmids pET21b-ARF6 and pBB131 were generously provided by Drs. F. Luton and M. Franco (IPMC-CNRS, Valbonne, France) (40).

Protein Expression and Purification—All the plasmids were transformed into Escherichia coli strain BL21(DE3)pLysS. Protein expression was induced overnight at 37 °C with 0.5 mM isopropyl β-D-1-thiogalactopyranoside. Bacteria were centrifuged and lysed by sonication. Purification of His$_6$-tagged recombinant proteins was carried out under native conditions in accordance with the protocol specified by Qiagen, except that the purification buffers contained 20 mM Tris-HCl, pH 7.4, instead of 50 mM phosphate, pH 8; NaCl was 300 mM; the lysis buffer contained 8 –10 mM imidazole; the washing buffer contained 20 mM imidazole; and the elution buffer contained 250 or 400 mM imidazole. GST-fused recombinant proteins were purified on glutathione-Sepharose beads following standard procedures, except for pulldown assays, for which GST-RIM-RBD and GST-VHS-GAT bacterial lysates were frozen until use.

For recombinant myristoylated ARF6 expression and purification, BL21(DE3)pLysS bacteria were cotransformed with pET21b-ARF6 and pBB131, encoding yeast *N*-myristoyltransferase. Recombinant myristoylated ARF6 with a C-terminal hexahistidine tag was purified by adsorption to His-Bind resin (nickel-nitrilotriacetic acid-agarose, Qiagen) and elution with 200 mM imidazole, pH 8 (40). Myristoylation was confirmed by Triton X-114 partitioning as described previously (38). When indicated, myr-ARF6 was loaded for 1 h at 37 °C with 0.125 mM of the appropriate guanosine nucleotide (GDPβS, GTPγS, or GDP) in a buffer containing 5 mM MgCl$_2$, 0.03% Nonidet P-40, 1 mM DTT, 25 mM EDTA, and 50 mM HEPES potassium salt, pH 7.2. ARF6 was separated from free nucleotides by gel filtration in Sephadex G-25 minicolumns equilibrated in PBS containing 1% BSA and 1 mM MgCl$_2$. The purified protein was stored at −20 °C until use.

SDS-PAGE and Immunoblotting—Proteins were separated on Tris-Tricine-SDS gels (41) and transferred to 0.22-μm nitrocellulose membranes (Hybond; GE Healthcare). Nonspecific binding was blocked with 5% nonfat dry milk dissolved in washing buffer (0.1% Tween 20 in PBS) for 1 h at room temperature. Blots were incubated with 0.5 μg/ml mouse monoclonal anti-ARF6 antibody (Abcam ab19871), 0.2 μg/ml mouse monoclonal anti-Rab3A antibody, or 0.2 μg/ml anti-α-tubulin in blocking buffer for 2 h. After washing three times, blots were incubated with 0.25 μg/ml HRP-conjugated anti-mouse antibody in washing solution for 1 h and washed three times. Detection was accomplished with Western Lightning Chemiluminescence Reagent Plus (PerkinElmer Life Sciences). The images of the bands were obtained using a Luminescent Image Analyzer LAS-4000 (Fujifilm, Tokyo Japan).

Triton X-114 Partition—Partition experiments were conducted following standard procedures (38). In brief, capacitated sperm (50 × 10^6 cells) were washed twice with cold PBS, and proteins were extracted in 1 ml of lysis buffer (20 mM Tris-HCl, pH 7.5, 150 mM NaCl, 10% glycerol, 5 mM MgCl$_2$, and 1% Triton X-114) by sonication on ice (three times for 15 s each, with a 10-s interval). The lysates were rocked for 45 min at 4 °C and centrifuged at 14,000 × g for 20 min at 4 °C. The whole cell detergent extracts were then incubated for 15 min at 30 °C. The particulate fractions obtained after subcellular fractionation were dissolved in ice-cold lysis buffer and the protease inhibitor mixture by incubation for 15 min at 30 °C. The supernatants were added to Triton X-114 (1% final concentration) and incubated for 15 min at 37 °C. Samples were centrifuged at 3000 × g for 3 min at room temperature. Hydrophilic proteins partitioned into the upper (aqueous) phase, whereas hydrophobic proteins were recovered from the lower (detergent) phase. Protein precipitation and removal of detergent were achieved via extraction with CCl$_3$H-CH$_3$OH-H$_2$O. Precipitated proteins were dissolved in sample buffer by heating at 95 °C for 3 min.

Indirect Immunofluorescence—3.5 × 10^5 sperm cells were spotted on poly-L-lysine-coated coverslips and fixed with 4% paraformaldehyde in PBS. Free aldehyde groups were quenched with 50 mM glycine in PBS, and sperm were permeabilized with 0.1% Triton X-100 in PBS. Nonspecific reactivity was blocked with 5% BSA. Coverslips were incubated overnight at 4 °C with 10 μg/ml mouse monoclonal anti-ARF6 antibody (ab131261) diluted in 1% BSA in PBS. After three washes with PBS, cells were incubated 1 h at room temperature with 2 μg/ml anti-mouse Cy3-conjugated antibody in 1% BSA in PBS. Excess of secondary antibody was washed three times with PBS. Finally, cells were fixed for 1 min in cold methanol and double-stained with FITC-PSA as described below under "Acrosome Reaction Assay." After this procedure, slides were mounted in 1% propyl gallate, 50% glycerol in PBS. Sperm staining patterns were analyzed with an Olympus FV1000 confocal microscope.

Acrosome Reaction Assay—Human semen samples were obtained from healthy volunteer donors. The informed consent signed by the donors and the protocol for semen sample handling were approved by the Ethic Committee of the School of Medicine, National University of Cuyo. We are cognizant of the Argentinean (ANMAT 5330/97) and international (Declaration of Helsinki) principles and bioethical codes, and we guar-

antee that all procedures carried out in conducting the research reported here were in compliance with both.

Highly motile sperm were recovered after a swim-up separation for 1 h in HTF (5.94 g/liter NaCl, 0.35 g/liter KCl, 0.05 g/liter $MgSO_4 \cdot 7H_2O$, 0.05 g/liter KH_2PO_4, 0.3 g/liter $CaCl_2 \cdot 2H_2O$, 2.1 g/liter $NaHCO_3$, 0.51 g/liter glucose, 0.036 g/liter sodium pyruvate, 2.39 g/liter sodium lactate, 0.06 g/liter penicillin, 0.05 g/liter streptomycin, 0.01 g/liter phenol red supplemented with 5 mg/ml of BSA) at 37 °C in an atmosphere of 5% CO_2, 95% air. Cell concentration was then adjusted with HTF to $5–10 \times 10^6$ sperm/ml. To promote capacitation of the motile fraction recovered from the swim-up procedure, sperm were incubated in HTF supplemented with 5 mg/ml bovine serum albumin for at least 3 h at 37 °C in an atmosphere of 5% CO_2, 95% air.

Capacitated spermatozoa were permeabilized by incubating with 2.1 units/ml SLO in HB-EGTA (20 mM HEPES potassium salt, 250 mM sucrose, 0.5 mM EGTA, pH 7) as described previously (33, 42). Inhibitors or stimulants were added as indicated in the figure legends. Samples for each condition were air-dried, fixed/permeabilized with −20 °C methanol, and stained with 50 μg/ml FITC-PSA in PBS for 40 min at room temperature (42). Then the cells were washed with distilled water for 20 min at 4 °C. At least 300 cells were scored using a Nikon microscope equipped with epifluorescence optics. Negative (no stimulation) and positive (stimulated with 0.5 mM $CaCl_2$ corresponding to 10 μM free calcium estimated by MAXCHELATOR) controls were included in all experiments. For each experiment, acrosomal exocytosis indexes were calculated by subtracting the number of reacted spermatozoa in the negative control (range 6.6–22%) from all values and expressing the resulting values as a percentage of the acrosome reaction observed in the positive control (range 15–45%). The average difference between positive and negative control was 14% (experiments where the difference was <10% were discarded). In short, we will mention this technique in the text as classical or indirect method.

Real Time Acrosomal Exocytosis Measurements (Direct Method)—SLO-permeabilized human sperm (5×10^6 cells/ml) were immobilized in poly-L-lysine (0.01%) pre-coated cover slides. Samples were mounted in a chamber at 37 °C, and the medium was supplemented with 5 μg/ml FITC-PSA. The AR was induced by adding myr-GTPγS-ARF6 (400 nM). Images were recorded during 10 min in an Olympus FV1000 confocal microscope. Analysis of images was performed using the software ImageJ (Wayne Rasband, National Institutes of Health).

Acrosomal Exocytosis Measurements by Using Flow Cytometry (Direct Method)—SLO-permeabilized sperm (5×10^6 cells/ml) suspended in HB-EGTA supplemented with 5 μg/ml FITC-PSA were stimulated with 400 nM myr-GTPγS-ARF6 or 200 nM PMA for 15 min at 37 °C. Control condition corresponds to sperm incubated in HB-EGTA/FITC in the absence of any stimulation. Cells were fixed with 2% paraformaldehyde in PBS, and an aliquot of the preparation was analyzed (10,000 events) in a FACSAria III cytometer (BD Biosciences). The data were analyzed by FlowJo software. To evaluate the staining patterns of sperm populations, cells were sorted by FACS, and confocal images of sperm were obtained. We used an Olympus

FV1000 confocal microscope. Analysis of images was performed using the software Image J (Wayne Rasband, National Institutes of Health).

Lipids Added to Spermatozoa—For diacylglycerol, 100 mM DAG in DMSO stock solution was kept at −20 °C until used. Successive dilutions in HB-EGTA were done to reach a final DAG concentration of 0.5 mM. One μl of the 0.5 mM solution was added to 49 μl of sperm suspension in HB-EGTA to get a final concentration of 10 μM. The final DMSO concentration was 0.01%.

Phorbol Ester—1 M PMA stock in DMSO was prepared, and a N_2 stream was applied before storing at −20 °C. We added 0.5 μl of the stock to 49.5 μl of DMSO to obtain a 0.01 M solution. From this stock, we prepared additional dilutions in HB-EGTA until getting a 10 μM PMA solution. One μl of the 10 μM stock was added to 49 μl of sperm suspension to get a final concentration of 200 nM.

Phosphatidic Acid—5 mM PA in DMSO stock solution was kept at −20 °C until used. A dilution in HB-EGTA was done to reach a concentration of 0.5 mM. One μl of the 0.5 mM solution was added to 49 μl of sperm suspension in HB-EGTA to get a final concentration of 10 μM PA. The final DMSO concentration was 0.2%.

Phosphatidylinositol 4,5-bisphosphate was dissolved in chloroform/methanol/water (20:9:1, v/v), vortexed, and evaporated. The lipid was then dissolved in chloroform and dried under a nitrogen stream. PIP_2 is a polar phospholipid with a variable net charge (subject to pH and membrane interactions) that forms micelles in aqueous solution. PIP_2 micelles were made by suspending the lipid in HB-EGTA at a final concentration of 2.5 mM (stock solution), followed by several minutes of sonication at maximum power. One μl of the 2.5 mM solution was added to 49 μl of sperm suspension in HB-EGTA to get a final concentration of 50 μM PIP_2.

PLD Activity Measurements—SLO-permeabilized sperm were adjusted to 100,000 cells/condition in HB-EGTA medium and incubated with 100 μM 2-APB for 15 min at 37 °C (to prevent exocytosis). Cells were further incubated with 10 μM free calcium, 10 μM DAG or 400 nM myr-GTPγS-ARF6 for 15 min at 37 °C. Basal PLD activity was measured without addition of any stimulus. The medium was replaced by 100 μl of ice-cold Tris 50 mM, pH 8.0, and the cells were lysed by sonication. Samples were collected and mixed with an equal amount of Amplex Red reaction buffer (Amplex Red phospholipase D assay kit, Molecular Probes), and the PLD activity was estimated after 1 h of incubation at 37 °C with a Mithras fluorometer (Berthold). A standard curve was established with purified PLD from *Streptomyces chromofuscus* (Sigma).

Thin Layer Chromatography (TLC)—5×10^7 cells/condition were permeabilized with SLO and treated with 1 mM $MgCl_2$ to stimulate kinase activity, 5 mM NaF to avoid phosphatase activity, and 15 μM U73122 to prevent PIP_2 hydrolysis. To evaluate PIP_2 synthesis, 0.375 μCi of [γ-^{32}P]ATP was added to each aliquot, and cells were kept under control conditions or stimulated with 10 μM free calcium or 400 nM myr-GTPγS-ARF6. Lipids were neutralized with 1 volume 1 M HCl and extracted with 2 volumes methanol/chloroform (1:1). Phosphoinositides were then resolved on TLC plates with chloroform/acetone/

methanol/acetic acid/H_2O (80:30:26:24:10) and visualized by autoradiography.

PLC Activity Measurements—[γ-^{32}P]PIP$_2$ was synthesized *in vitro* by adding 0.4 μg of GST-PIPKIγ-5 and 10 μCi of [γ-^{32}P]ATP to 50 μl of reaction buffer (50 mM Tris-HCl, pH 7.5, 1 mM EGTA, 10 mM MgCl$_2$, 80 μM phosphatidylinositol 4-phosphate (PI4P)). The mixture was incubated for 20 min at room temperature as described in Wang and Sugita (37). The reaction was stopped by the addition of 100 μl of 1 N HCl, and [γ-^{32}P]PIP$_2$ was then extracted with 200 μl of chloroform/methanol (1:1). The phospholipid isolated was resuspended in 80 μl of HB-EGTA, and 20 μl were added to each aliquot of SLO-permeabilized sperm. Cells were kept under control conditions or stimulated with 10 μM DAG or 400 nM myr-GTPγS-ARF6 for 15 min at 37 °C. When indicated, 1 μM C1 domain of Munc13-1 was added before the ARF6 stimulus. Lipids were neutralized with 1 volume of 1 M HCl and extracted with 2 volumes of methanol/chloroform (1:1). Phosphoinositides were then resolved on TLC plates with chloroform/acetone/methanol/acetic acid/H_2O (80:30:26:24:10) and visualized by autoradiography.

Imaging of Intracellular Calcium Stores—SLO-permeabilized sperm were incubated for 30 min at 37 °C in the presence of 2 μM Fluo3-AM. The cells were then washed with HB-EGTA. Afterward, cells were immobilized on poly-L-lysine-coated round coverslips (0.01% w/v poly-L-lysine drops were air-dried followed by one rinse with water), which were mounted on a chamber and placed on the stage of an inverted Eclipse TE300 Nikon microscope. LED output was synchronized to the Exposure Out signal of a Luca R EMCCD camera (Andor Technology, UK). Images were collected (three frames/s) using NIS Element software (Nikon, New York) and a Plan Apo $\times$60/1.40-oil Nikon objective. Images were processed using ImageJ. Any incompletely adhered sperm that moved during the course of the experiment was discarded. Fluorescence measurements in individual sperm were made by manually drawing a region of interest around the acrosome and midpiece of each cell. Results are presented as pseudo color [Ca^{2+}]$_i$ images as indicated on the figures. When required, raw intensity values were imported into Microsoft Excel and normalized using F/F_o, where F is fluorescence intensity at time t, and F_o is the mean of F taken during the control period. The total series of F/F_o were then plotted *versus* time (seconds). Relative fluorescence (%) is the fluorescence normalized to that obtained before the ARF6 protein addition.

GST Pulldown Assay—SLO-permeabilized sperm (30 $\times$ 10^6 cells) were treated with 100 μM 2-APB, loaded with 10 nM (0.25 ng) His$_6$-GDP-Rab3A (Fig. 10) or 10 nM His$_6$-GDP-ARF6 (Fig. 11) for 15 min at 37 °C. Then, in Fig. 10, cells were challenged with 10 μM DAG or 400 nM myr-ARF6-GTPγS and in Fig. 11 with 10 μM free calcium or 300 nM PMA. After 15 min of incubation at 37 °C, cells were lysed by sonication on ice in GST pulldown buffer (200 mM NaCl, 2.5 mM MgCl$_2$, 1% (v/v) Triton X-100, 10% glycerol, 1$\times$ protease inhibitor mixture (P2714, Sigma), and 50 mM Tris-HCl, pH 7.4). The sonication was repeated twice for 15 s. These whole cell detergent extracts were clarified by centrifugation at 12,000 $\times$ g for 5 min and used immediately. Glutathione-Sepharose beads were washed twice

with GST pulldown buffer and incubated with bacterial lysates containing GST-RIM-RBD (Fig. 10) or GST-VHS-GAT (Fig. 11) for 1 h at 4 °C under constant rocking. Beads were washed twice with PBS and once with GST pulldown buffer and used immediately. 20 μl of glutathione-Sepharose containing 10 μg of the GST-RIM-RBD or 10 μg of the GST-VHS-GAT was added to sperm lysates prepared as described above and incubated by rotation at 4 °C for 45 min. The resin was recovered by centrifugation at 4 °C and washed three times with ice-cold GST pulldown buffer. The resin-bound fractions were boiled in sample buffer and resolved by SDS-PAGE, and Rab3A-GTP or ARF6-GTP levels were analyzed by immunoblotting as described under "SDS-PAGE and Immunoblotting."

Detection of Nucleotide Binding Status of Endogenous Rab3—Capacitated and permeabilized sperm were incubated with 100 μM 2-APB for 10 min at 37 °C to prevent acrosomal loss due to exocytosis. The AR was induced with 10 μM free calcium, 10 μM DAG, or 400 nM ARF6 for 15 min at 37 °C. Following this step, cell suspensions were fixed in 2% paraformaldehyde, neutralized with 100 mM glycine, attached to poly-L-lysine-coated coverslips, and stored overnight at 4 °C in a moisturized chamber. Sperm were permeabilized with 0.1% Triton X-100 in PBS for 10 min at room temperature; cells were washed three times (6 min each) with PBS, 0.1% poly(vinylpyrrolidinone) (PVP), and nonspecific reactivity was blocked in 5% BSA in PBS, 0.1% PVP, for 1 h at 37 °C. Slides were overlaid with 140 nM GST-RIM-RBD in 3% BSA in PBS, 0.1% PVP, for 1 h at 37 °C. After washing (three times, 6 min each, PBS, 0.1% PVP), anti-GST antibodies (31.5 μg/ml = 210 nM, in 3% BSA in PBS/PVP) were added to the coverslips, and incubated for 1 h at 37 °C in a moisturized chamber. After washing twice for 10 min with PBS, we added Cy3-conjugated goat anti-rabbit IgG (1.67 μg/ml in 1% BSA in PBS, 0.1% PVP) and incubated for 1 h at room temperature protected from light. Coverslips were washed six times for 6 min each with PBS, 0.1% PVP. Cells were subsequently stained for acrosomal contents as described before but without air drying, mounted with 1% propyl gallate, 50% glycerol in PBS containing 2 μM Hoechst 33342, and stored at −20 °C in the dark until examination as described under "Indirect Immunofluorescence." We scored the presence of immunostaining in the acrosomal region by manually counting between 100 and 200 cells either directly at the fluorescence microscope. Data were evaluated using the Tukey-Kramer post hoc test for pairwise comparisons.

Statistical Analysis—Differences between conditions were tested by one-way analysis of variance and post hoc tests like Tukey-Kramer's or Dunnett's. When specified in legends to figures, Student's single group t test was used.

RESULTS

ARF6 Is Present in Human Sperm Cells and Is Required for Calcium- and DAG-induced Acrosomal Exocytosis—Given that ARF6 regulates the concentration of PIP$_2$ and PA in other cells (11, 14), we asked whether ARF6 is present in human sperm and whether it is required for calcium- and DAG-induced exocytosis. The presence of ARF6 in human sperm was first investigated by Western blot using a specific monoclonal antibody raised against purified recombinant full-length human ARF6.
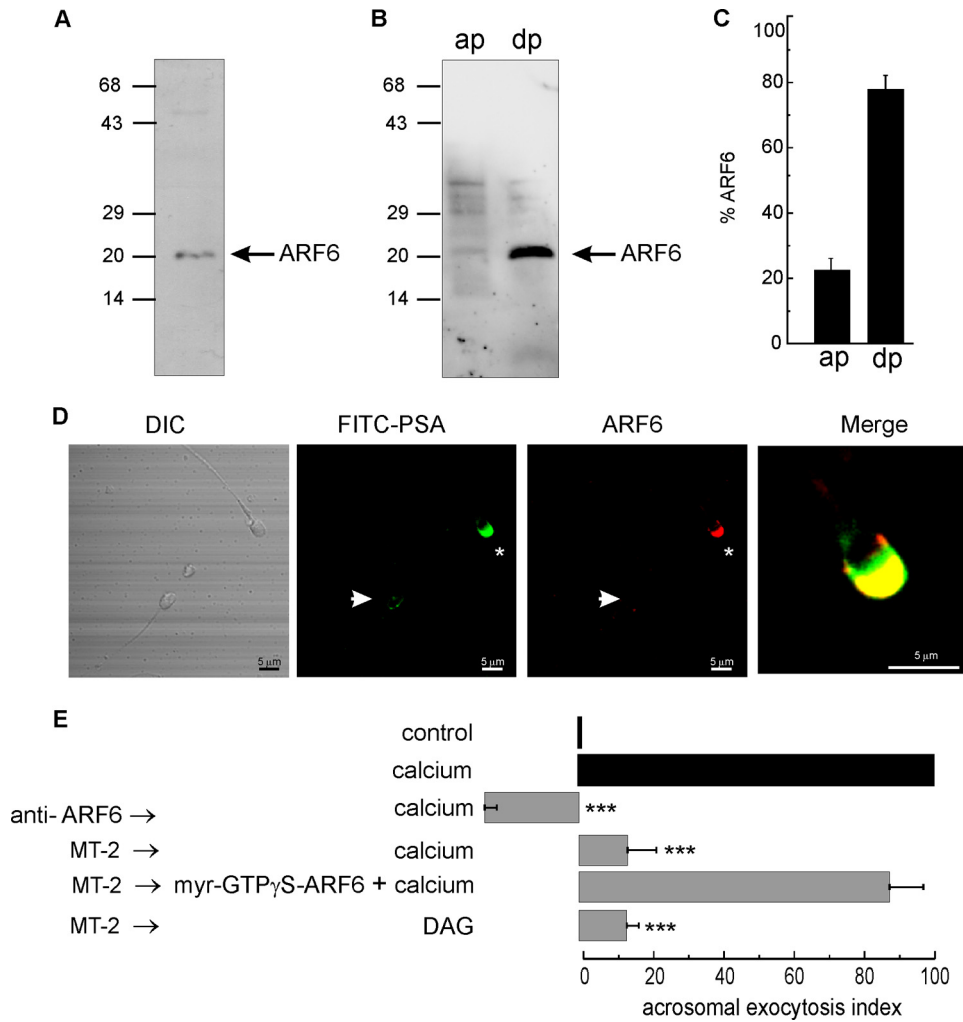
FIGURE 1. **ARF6 is present in human sperm and is required for calcium- and DAG-induced AR.** *A*, membranes from 40×10^6 sperm cells were obtained according to Bohring and Krause (93). The samples were analyzed by Western blot using the anti-human ARF6 antibody. Molecular mass standards (kDa) are indicated to the *left*. *B*, whole sperm homogenates were partitioned in Triton X-114. Proteins from the aqueous (*aq*) and detergent phases (*dp*) were analyzed by Western blot. *C*, quantification of endogenous ARF6 partitioned in Triton X-114. Data shown are representative of three independent experiments. Quantification was carried out using ImageJ and expressed as percentage of ARF6 detected in each fraction. *D*, indirect immunofluorescence. Human spermatozoa were fixed and double-stained with rabbit polyclonal anti-human ARF6 antibody/Cy3-conjugated anti-rabbit antibody and FITC-PSA to differentiate between reacted (*arrow*) and nonreacted (*asterisk*) sperm. In the *merge image*, the *yellow-orange* staining indicates the areas of co-localization. *DIC*, differential interference contrast. *E*, SLO-permeabilized spermatozoa were incubated for 15 min at 37 °C with 20 μg/ml anti-ARF6 antibody or 300 nM MT-2. The samples were further incubated for 15 min at 37 °C in the presence of 0.5 mM CaCl₂ (*anti-ARF6/MT-2 → calcium*) or 10 μM DAG (*MT-2 → DAG*). When indicated, the sample was treated with 400 nM myr-GTPγS-ARF6 plus calcium after MT-2 incubation (*MT-2 → myr-GTPγS-ARF6 + calcium*). Controls were included (*black bars*): permeabilized sperm incubated in HB-EGTA without addition of any reagent (*control*) or supplemented with 0.5 mM CaCl₂ (10 μM free calcium). Sperm were fixed, and AR was evaluated by FITC-PSA binding. The data represent the mean ± S.E. from 3 to 11 independent experiments. Dunnett's test was used to compare the means of all groups against the calcium-stimulated condition in the absence of inhibitors. Significant differences (***, $p < 0.001$) are indicated for each bar. Differences were considered not significant at the $p > 0.05$.

As shown in Fig. 1*A*, the anti-ARF6 antibody recognized a single protein band in sperm membrane subcellular fraction with an apparent molecular mass of ~20 kDa, coincident with that of the purified human recombinant ARF6 (data not shown). We inferred that ARF6 is myristoylated in sperm because it partitioned almost entirely (80%) into the detergent phase after Triton X-114 phase separation (Fig. 1, *B* and *C*). To determine its subcellular localization, we performed indirect immunofluorescence on fixed cells and double labeling with fluorescein isothiocyanate-conjugated *P. sativum* agglutinin (FITC-PSA), to distinguish between reacted (Fig. 1*D*, *arrow*) and nonreacted (Fig. 1*D*, *asterisk*) spermatozoa. Ninety percent of the nonreacted cells showed an acrosomal pattern of staining for ARF6, expected of a protein with a role in exocytosis. Acrosomal loss,

due to spontaneous exocytosis, generated a lack of FITC-PSA and ARF6 staining (Fig. 1*D*, *arrow*).

To assess whether ARF6 was implicated in calcium-induced AR, we performed exocytosis assays. To do so, we introduced an anti-ARF6 antibody into SLO-permeabilized human sperm and monitored its effect on the calcium-triggered AR. The antibody blocked calcium-induced exocytosis suggesting that the small GTPase is required for AR to proceed. To determine whether the active form of ARF6 was required for the AR, we resorted to a probe, MT-2, previously shown to interact specifically with GTP-bound ARF6 *in vitro* (43) and *in vivo* (11). Calcium or DAG was unable to achieve exocytosis in the presence of MT-2 (Fig. 1*E*), indicating that ARF6-GTP was necessary for acrosomal exocytosis. To confirm the specific binding of MT-2
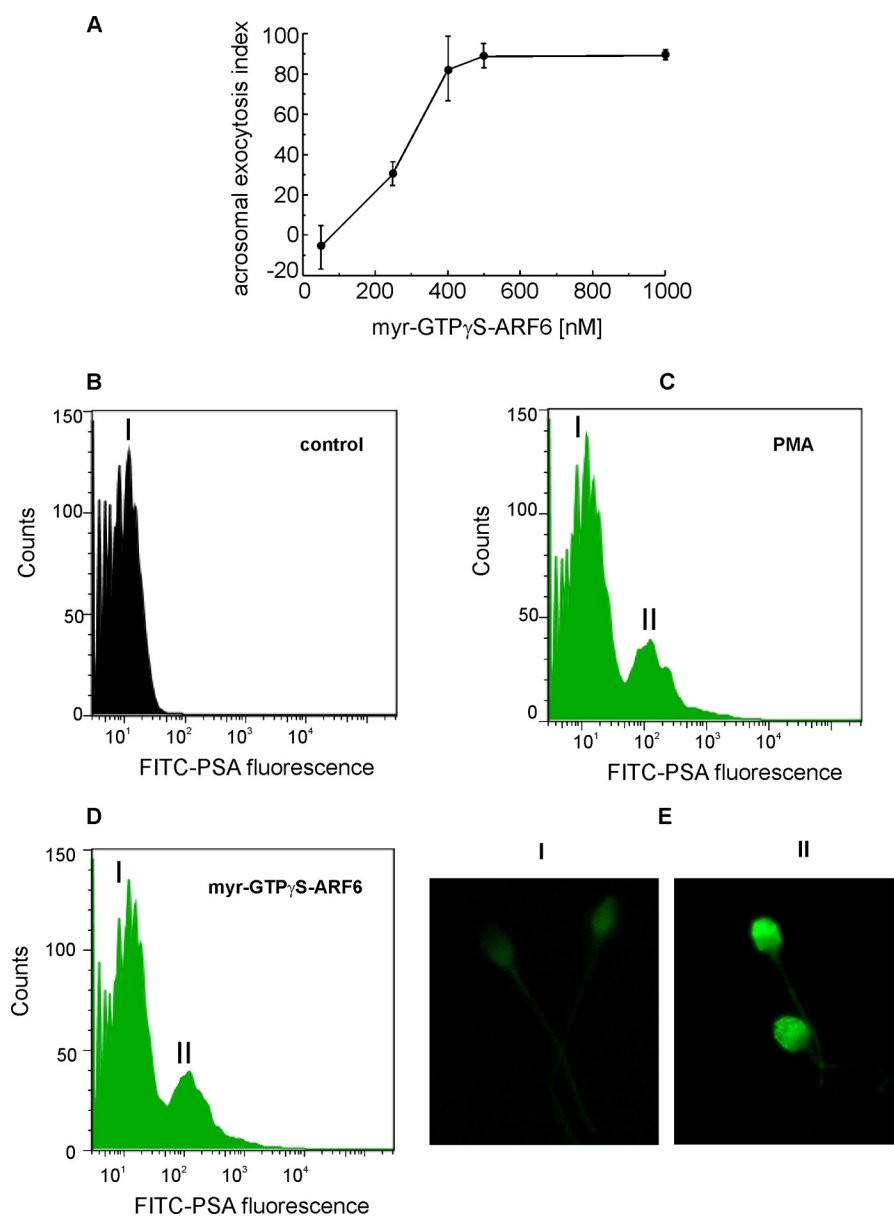
FIGURE 2. **Myristoylated and GTP-loaded ARF6 induces AR in a cytosolic calcium-independent manner.** *A,* SLO-permeabilized sperm were incubated for 15 min at 37 °C with increasing concentrations of myr-GTPγS-ARF6 (50–1000 nM). *B–D,* measurement of the AR by a direct method using flow cytometry. Permeabilized human sperm (5×10^6 cells/ml) were incubated at 37 °C in HB-EGTA supplemented with 5 µg/ml FITC-PSA in the absence of any reagent (*control, B*), or stimulated with 300 nM PMA (*PMA, C*) or 400 nM myr-GTPγS-ARF6 (*myr-GTPyS-ARF6, D*). 10,000 cells were sorted by FACS according to FITC-PSA fluorescence. *Graphs* of a representative experiment showing the number of FITC-PSA stained cells (*counts*) *versus* FITC-PSA fluorescence intensity. Note the sperm population with increased fluorescence that appeared upon incubation with a stimulus. *E,* images of cells sorted by FACS correspond to nonreacted sperm (*panel I, left*) and reacted sperm (*panel II, right*).

to active ARF6, we rescued the MT-2 inhibition by the addition of recombinant myristoylated and GTP-loaded ARF6 before calcium stimulus (Fig. 1*E*). Taken together, these data demonstrate that myristoylated ARF6 is present in and localizes to the acrosomal region of human sperm and suggest that active ARF6 is required for calcium- and DAG-induced AR.

Myristoylated and GTP-loaded ARF6 Induces Acrosomal Exocytosis in an External Calcium-independent Manner—We have demonstrated that PIP$_2$ increases its concentration upon calcium or DAG exocytic stimuli and that PA is able to induce sperm PIP$_2$ synthesis. However, neither PA nor PIP$_2$ are able to trigger exocytosis by themselves (33). Therefore, if ARF6 is only modifying lipid concentration in membranes, we predict that

active ARF6 will not affect exocytosis *per se*. Surprisingly, when permeabilized cells were challenged with increasing concentrations of myristoylated and GTPγS-loaded ARF6 (myr-GTPγS-ARF6), they underwent acrosomal exocytosis in a dose-dependent fashion (Fig. 2*A*). The percentage of cells showing exocytosis increased with the GTPase concentration, reaching a maximum at 400 nM.

The FITC-PSA method is used routinely to assess the state of the acrosomes in fixed and permeabilized sperm; because it stains the acrosome after fixation, we refer to it as an "indirect staining method" (44, 45). To evaluate with accuracy the percentage of cells responding to active ARF6 stimulation, we used flow cytometry and real time measurements by confocal microscopy, in addition
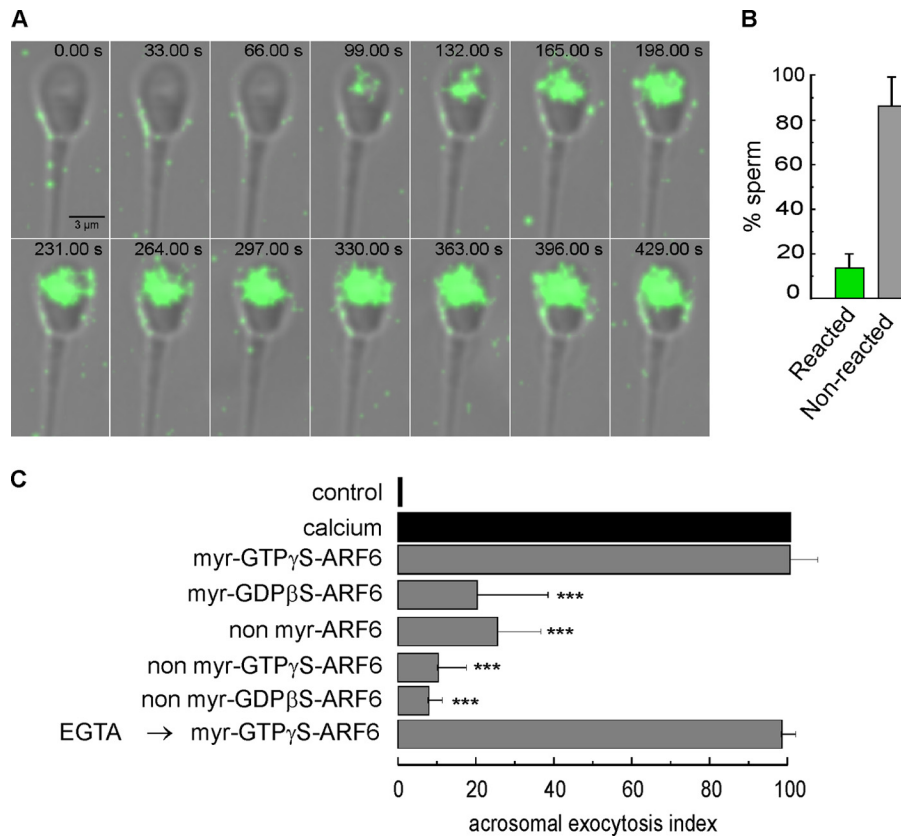
FIGURE 3. **Myristoylated and GTP-loaded ARF6 induces AR in a cytosolic calcium-independent manner.** Visualization of the AR in real time by confocal microscopy. *A*, real time fluorescence imaging of acrosomal exocytosis in human sperm. Human sperm were stimulated with 400 nm myr-GTPγS-ARF6 in HB-EGTA supplemented with 5 μg/ml FITC-PSA and recorded at two frames/min during 10 min in a confocal microscope. *B*, percentage of reacted and nonreacted sperm recorded by real time. The data represent the mean ± S.E. from 3 to 11 independent experiments. *C*, sperm were permeabilized with SLO and incubated in the media without any reagent addition (*control*) or with 10 μM of free calcium (*calcium*) or 400 nm of myr-GTPγS-ARF6, myr-GDPβS-ARF6, non-myr-ARF6, non-myr-GTPγS-ARF6, and non-myr-GDPβS-ARF6 at 37 °C for 15 min (*gray bars*). When indicated, cells were treated before the stimulus with 5 mm EGTA for 15 min at 37 °C (*EGTA → myr-GTPγS-ARF6*). The data represent the mean ± S.E. from 3 to 6 independent experiments. Dunnett's test was used to compare the means of all groups against the calcium-stimulated condition in the absence of inhibitors. Significant differences (***, $p < 0.001$) are indicated for each *bar*. Differences were considered not significant at the $p > 0.05$.

to the conventional static method. We set up and adapted to permeabilized sperm a method described recently by Zoppino *et al.* (46) for nonpermeabilized sperm. Permeabilized cells were incubated in the presence of FITC-PSA before adding the stimuli. PSA-FITC is incorporated into the acrosome during exocytosis staining the acrosome (direct method). The granule remains fluorescent for an extended period of time. We scored the number of fluorescent cells by flow cytometry. We observed one peak (Fig. 2*B*, *black area*) when permeabilized cells were incubated in the buffer without any additional treatment (negative control). Upon challenging sperm with 400 nm myr-GTPγS-ARF6 or 200 nm PMA, a DAG analogue known to induce the AR (33), we observed a shift in the fluorescence pattern and detected an additional population of brightly fluorescent cells (two peaks, Fig. 2, *C* and *D*, *green area*). To validate this method, we analyzed in a fluorescence microscope the staining pattern of the populations obtained by cell sorting. Peak I (Fig. 2, *B–D*, *black area*) represented nonreacted cells and showed slight fluorescence (Fig. 2*E*, *peak I*). The reacted pattern (*peak II*, Fig. 2, *C* and *D*) showed strong fluorescence at the acrosomal region of the sperm head (Fig. 2*E*, *peak II*). The population of reacted cells after ARF6 stimulus scored by flow cytometry ranged between 10 and 16%. This percentage is similar to that observed with physiological stimuli (progesterone and zona pellucida).

Because of routine use, versatility, and suitability, most of the experiments presented here were carried out using the indirect method. It also provides reliable results that are easy to interpret and offers a rapid technique for evaluating AR. Even so, we confirmed these results by flow cytometry (data not shown).

Next, the effect of myr-GTPγS-ARF6 on sperm acrosome exocytosis in permeabilized cells was monitored in real time by confocal microscopy. Permeabilized cells were incubated in the presence of FITC-PSA and stimulated with 400 nm myr-GTPγS-ARF6. The cells were then analyzed by time-lapse imaging in a confocal microscope. An increase in fluorescence was observed when active ARF6 was added (starting between 1.30 and 4 min post-addition, Fig. 3*A* and supplemental Video 1). The absolute percentage of sperm that underwent AR measured by this method (Fig. 3*B*) was similar to those observed by flow cytometry and in fixed cells using the conventional technique.

We conclude that incubation of permeabilized sperm with 400 nm myr-GTPγS-ARF6 triggers exocytosis as efficiently as calcium and PMA (Figs. 2 and 3, *A* and *B*). The effect was observed in the absence of external calcium given that free calcium concentration in the buffer, which contains 0.5 mm EGTA, is in the 100 nm range (Figs. 2 and 3*A*). When 5 mm EGTA was added to the medium, the free calcium concentration dropped to less than 10 nm (47). At these very low calcium
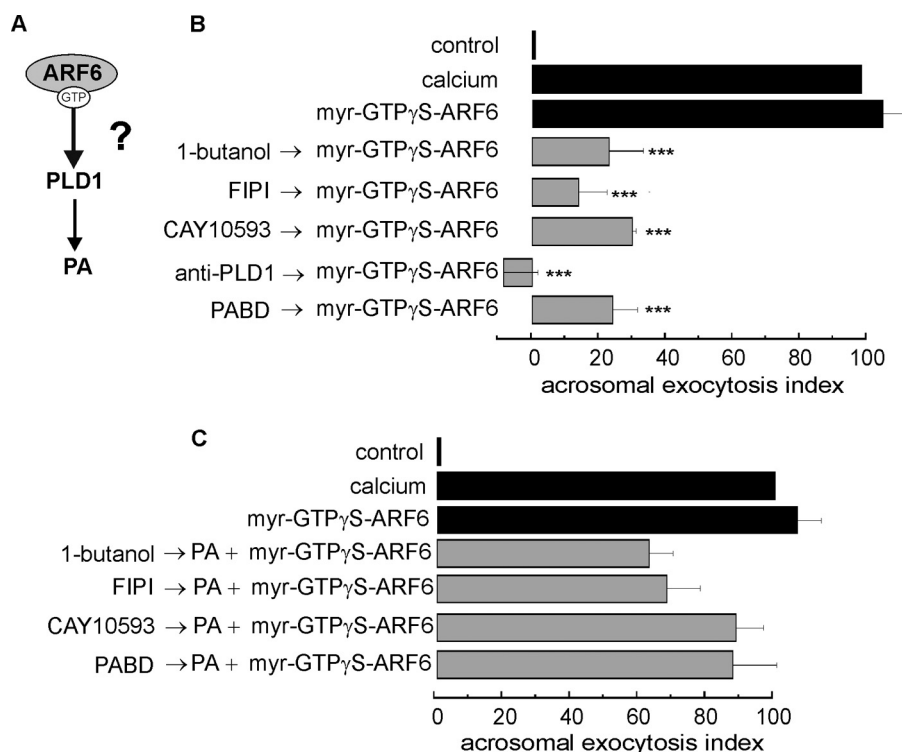
FIGURE 4. **Active ARF6-induced sperm exocytosis requires PLD activity.** *A,* scheme depicting the hypothesis of ARF6-induced signaling pathway in acrosomal exocytosis. Does ARF6 require PLD1 activity during AR? *B,* SLO-permeabilized sperm were incubated with the following compounds affecting PLD activity, 0.5% 1-butanol, 10 nM FIPI, 50 nM CAY10593, 20 μg/ml anti-PLD1 antibody, or 10 μg/ml PABD for 15 min at 37 °C. The samples were further incubated for 15 min at 37 °C in the presence of 400 nM myr-GTPγS-ARF6. Several controls were included (*black bars*): permeabilized sperm incubated in HB-EGTA alone (control) or with the addition of the following reagents: 0.5 mM CaCl$_2$ (10 μM free calcium, estimated by MAXCHELATOR) or 400 nM myr-GTPγS-ARF6. *C,* SLO-permeabilized sperm were treated with reagents affecting PLD activity and further incubated for 15 min at 37 °C in the presence of 400 nM myr-GTPγS-ARF6 plus 10 μM PA. The data represent the mean $\pm$ S.E. from three to eight independent experiments. Dunnett's test was used to compare the means of all groups against calcium-stimulated conditions. Significant differences (***, $p < 0.001$) are indicated for each *bar*. Differences were considered not significant at the $p > 0.05$.

concentrations, there was still a significant percentage of sperm that underwent exocytosis in response to ARF6 (Fig. 3*C*, *EGTA → myr-GTPγS-ARF6*). Under these conditions the active GTPase suffices to trigger exocytosis.

Post-translationally myristoylated ARF6 partitions in its GDP-bound state between the cytosol and a low affinity complex with membranes, whereas ARF6-GTP associates tightly with membranes. This stable interaction is mediated by the myristoylated N-terminal helix, which flips open upon binding GTP and inserts into the lipid bilayer. Therefore, this myristoylation is important for membrane targeting and is crucial for biological function (48). To determine whether myristoylation and activation of ARF6 were required for the effect of the recombinant protein, myristoylated or nonmyristoylated His$_6$-ARF6 was loaded with GTPγS or GDPβS (slowly hydrolyzable analogues of GTP and GDP, respectively) and incorporated into permeabilized cells. The myristoylation percentage of the recombinant protein used was ~80% determined by Triton X-114 phase separation (data not shown). The recombinant nonmyristoylated protein failed to induce exocytosis even when loaded with GTPγS (Fig. 3*C*). Only myristoylated and GTPγS-loaded ARF6 promoted secretion (Fig. 3*C*). These observations indicate that recombinant ARF6 must be in the same functional configuration as endogenous ARF6 proteins (*i.e.* myristoylated and in the GTP-bound form) to be active in exocytosis.

Active ARF6-induced Sperm Exocytosis Requires a PLD Activity—What molecular mechanism drives the ARF6-induced exocytosis? As stated previously, acrosomal exocytosis is

organized as a bifurcated pathway, with two separate limbs that diverge downstream of cAMP/Epac (28). The end point of one branch is the mobilization of intracellular calcium from internal stores through the activation of PLC via Rap, whereas the other branch (Rab3A-SNAREs) assembles the fusion protein machinery so that the outer acrosomal and plasma membranes become physically connected (protein branch). Both pathways operate in a concerted fashion and converge at/or downstream of intracellular calcium mobilization to accomplish exocytosis; once calcium is released into the cytosol, the protein machinery, likely through synaptotagmin (39), senses the rise in calcium concentration, and the whole system evolves to open the fusion pores. To trigger exocytosis, ARF6 should activate both limbs. We previously demonstrated that PLD1 is present and required for activating the branch that leads to acrosomal calcium efflux (33), and it has been reported that ARF6 regulates PLD activity in other cells (17). Having established that ARF6 is present in human sperm, is absolutely required for calcium- and DAG-induced AR, and that it triggers exocytosis, we wanted to know whether ARF6 requires and/or regulates PLD activity in this process (Fig. 4*A*). First, we analyzed whether PLD was required for ARF6-induced acrosomal exocytosis. It is well known that the PLD signaling pathway is disrupted in the presence of primary alcohols, because the enzyme catalyzes a transphosphatidylation reaction forming phosphatidyl alcohols at the expense of PA (49). 1-Butanol eliminated the ARF6-triggered AR in human spermatozoa (Fig. 4*B*), implying the

involvement of a PLD in this process. Additionally, the potent and specific PLD inhibitor, FIPI, abrogated ARF6-induced acrosomal exocytosis. Because both inhibitors act on PLD1 and PLD2, we used CAY10593, which at low concentrations acts as a specific, potent, and selective PLD1 inhibitor (50). ARF6-induced exocytosis was completely abolished in the presence of 50 nM CAY10593 (Fig. 4B), suggesting that PLD1 is the isoform required for ARF6-induced acrosomal exocytosis. In line with this model, a polyclonal anti-PLD1 antibody blocked ARF6-induced exocytosis (Fig. 4B). Furthermore, incubation with the PABD from the yeast protein Spo20p, which binds tightly to PA, efficiently inhibited the ARF6-triggered exocytosis (Fig. 4B). Finally, we found that PA efficiently rescued ARF6-induced exocytosis in the presence of PLD inhibitors (Fig. 4C), suggesting that PA synthesis is required for the GTPase-elicited AR. Together these results strongly suggest that PA synthesized by PLD1 is necessary for ARF6-induced acrosomal exocytosis.

Myristoylated and GTP-loaded ARF6 Promotes PLD Activity and PIP$_2$ Synthesis in Human Sperm—To assess the possibility that ARF6 activates both PLD and PI4P-5K during human sperm AR (Fig. 5A), we evaluated PLD and PI4P-5K activities. As shown in Fig. 5B, PLD activity was significantly increased in spermatozoa stimulated with calcium, DAG, or ARF6 compared with resting cells. DAG and ARF6 were more effective activators of PLD than calcium.

The second prediction to be tested was that PIP$_2$ production should increase in permeabilized sperm upon incubation with active ARF6 (Fig. 5A). Permeabilized sperm were incubated with [γ-^{32}P]ATP, and the incorporation of ^{32}P into phosphoinositides was evaluated by thin layer chromatography (TLC) in the presence of the PLC inhibitor U73122, to avoid PIP$_2$ hydrolysis. Calcium and ARF6 increased significantly the levels of PIP$_2$ compared with the control condition (Fig. 5, C and D). Notice that the levels of PIP$_2$ increased by ~2-fold in response to ARF6 treatment (Fig. 5D). In conclusion, ARF6 increases PLD activity and PIP$_2$ synthesis in human spermatozoa amplifying the PIP$_2$-mediated signal.

Myristoylated and GTP-loaded ARF6 Promotes PLC Activity in Human Sperm—Next, we reasoned that if active ARF6 is inducing exocytosis, it is somehow involved in the synthesis of DAG and IP$_3$ through the activation of a PLC (Fig. 6A). To assess this hypothesis, we started by performing exocytosis assays. To test whether ARF6 requires a signal transduction cascade involving the activity of PLC, we used the thiol-reactive PLC inhibitor U73122 (51). Fifteen μM U73122 completely abolished ARF6-induced exocytosis (Fig. 6B), whereas the inactive analogue U73343 was not able to inhibit the AR (Fig. 6B). Edelfosine, another PLC inhibitor, was also tested. This is a synthetic lysophospholipid analogue that selectively inhibits phosphatidylinositol PLC but does not inhibit phosphatidylcholine-specific phospholipases C or D (52). Edelfosine (0.5 μM) blocked ARF6-induced exocytosis (Fig. 6B) confirming that a phosphatidylinositol PLC is necessary in the GTPase-triggered pathway.

If treatment with active ARF6 leads to PLC activation and consequently to the synthesis of DAG, it is tempting to speculate that accumulation of the latter will trigger exocytosis (33). Thus, we predicted that sequestering DAG with the C1 domain
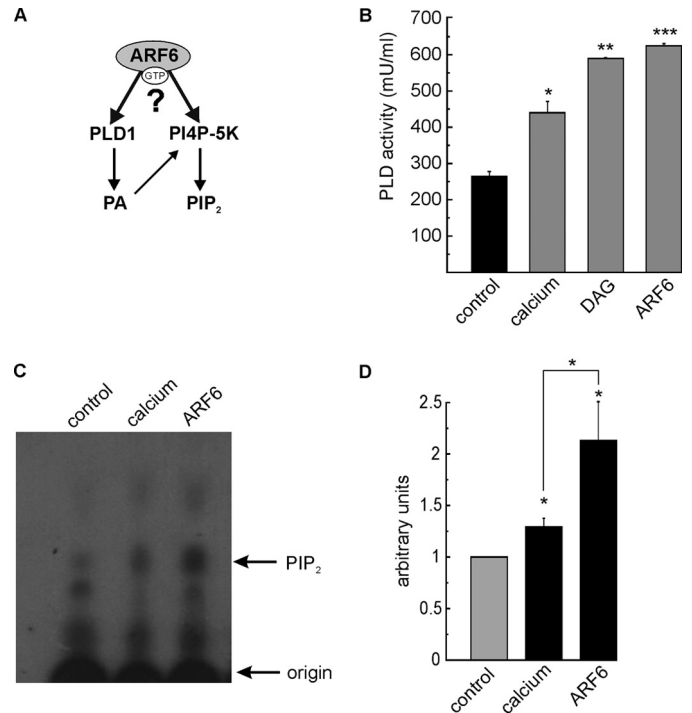

FIGURE 5. **Myristoylated and GTP-loaded ARF6 promotes PLD1 activity and PIP$_2$ synthesis in human sperm.** *A*, scheme depicting the hypothesis of ARF6-induced signaling pathway in acrosomal exocytosis. Is ARF6 activating PLD1 and PI4P-5K during AR? *B*, for PLD activity measurements, 100,000 cells/condition were incubated in HB-EGTA in the absence (*control*, *black bar*) or presence of 0.5 mM CaCl$_2$ (10 μM free calcium, *calcium*), 10 μM DAG, or 400 nM myr-GTPγS-ARF6 (*gray bars*) for 15 min at 37 °C. Spermatozoa were incubated with 100 μM 2-APB before the treatment to avoid AR. Cells were assayed for PLD activity. Data represent the mean values ± S.E. of four independent experiments. Dunnett's test was used to compare the means of all groups against the control condition in the absence of any stimulus. Significant differences are indicated for each bar (***, $p < 0.001$; **, $p < 0.01$; *, $p < 0.05$). *C*, 50 × 10^6 permeabilized spermatozoa were incubated with the PLC inhibitor U73122 (15 μM) for 15 min at 37 °C. After that, cells were incubated for an additional 15 min with 0.075 μCi of [γ-^{32}P]ATP with no additions (*control*) or stimulated with 10 μM free calcium or 400 nM myr-GTPγS-ARF6. Phospholipids were analyzed by TLC. *D*, quantification of the spot intensity (ImageJ). The values were normalized with respect to the control (mean ± S.E. of independent experiments). Significant increase of PIP$_2$ synthesis was assessed by *t* test for single group mean (*, $p < 0.05$).

of Munc13-1 would abolish ARF6-induced exocytosis. Therefore, we incubated permeabilized sperm with the C1 domain before myr-GTPγS-ARF6 was added. As predicted, the C1 domain inhibited the acrosomal exocytosis induced by the active GTPase (Fig. 6B). As a control, we confirmed that DAG-induced exocytosis was abolished when sperm were preincubated with the C1 domain. As demonstrated previously (33), calcium-induced exocytosis required DAG to occur (Fig. 6B). These results suggest that DAG synthesized by a PLC is responsible, at least in part, for ARF6-induced acrosomal exocytosis.

To directly prove that ARF6 affects PLC activity, we designed a strategy to measure changes in the enzyme activity in sperm. To this end, we first synthesized [^{32}P]PIP$_2$ *in vitro* as described by Wang and Sugita (37). We reasoned that if the small GTPase activates PLC, the addition of recombinant, active ARF6 to permeabilized sperm previously loaded with [^{32}P]PIP$_2$ will result in the hydrolysis of the phospholipid. The comparison of [^{32}P]PIP$_2$ spots by TLC was the readout of the hydrolysis suffered by the phospholipid after treatments. Results shown in
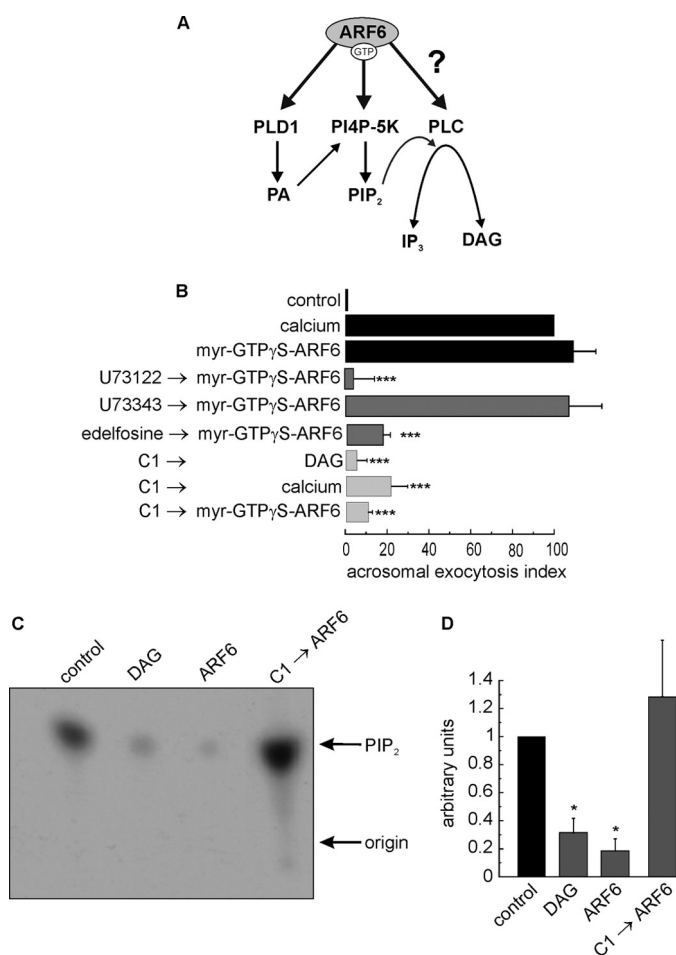
FIGURE 6. **Myristoylated and GTP-loaded ARF6 promotes PLC activity.** *A*, scheme depicting the hypothesis of ARF6-induced signaling pathway in acrosomal exocytosis. Is ARF6 able to activate a PLC during the AR? *B*, SLO-permeabilized spermatozoa were incubated for 15 min at 37 °C with 15 μM U73122, 15 μM U73343, 0.5 μM edelfosine, or 1 μM C1 domain of Munc13-1. When specified, AR was activated by adding 10 μM free calcium, 400 nM myr-GTPγS-ARF6, or 10 μM DAG for 15 min at 37 °C. Several controls were performed (*black bars*) as follows: sperm incubated in HB-EGTA (*control*) or HB-EGTA supplemented with 10 μM free calcium or 400 nM myr-GTPγS-ARF6. The data represent the mean $\pm$ S.E. from 3 to 10 independent experiments. Dunnett's test was used to compare the means of all groups against the calcium-stimulated condition. Significant differences (***, $p < 0.001$) are indicated for each *bar*. Differences were considered not significant at the $p > 0.05$. *C*, 50 $\times$ 10^6 permeabilized spermatozoa were incubated with [^{32}P] PIP$_2$ for 15 min at 37 °C. When specified, spermatozoa were loaded with 1 μM C1 domain. The samples were further incubated for 15 min at 37 °C in the presence of 10 μM DAG or 400 nM myr-GTPγS-ARF6. Phospholipids were analyzed by TLC. *D*, quantification of the spot intensity. The values were normalized with respect to the control (mean $\pm$ S.E. of four independent experiments). Significant PIP$_2$ hydrolysis was assessed by *t* test for single group mean (*, $p < 0.05$).

Fig. 6*C* confirmed the prediction; ARF6, as well as DAG, induced PIP$_2$ hydrolysis, indicating that both ARF6 and DAG promote PLC activity. The ARF6-induced decrease in [^{32}P]PIP$_2$ was abolished when permeabilized cells were preincubated with the PLC inhibitor U73122 (data not shown).

We wondered whether ARF6 activates a PLC directly or whether its effect is reinforced by DAG increase. To resolve this issue, we preincubated permeabilized cells with the C1 domain of Munc13-1 to sequester DAG. We then added [^{32}P]PIP$_2$ plus active ARF6 (Fig. 6*C*, *C1 $\rightarrow$ ARF6*). DAG sequestration before ARF6 treatment increased significantly the levels of [^{32}P]PIP$_2$ compared with the ARF6 condition. Taken together, our data

suggest that ARF6 stimulates PIP$_2$ synthesis (Fig. 5, *C* and *D*) and at the same time promotes PIP$_2$ hydrolysis mostly through a DAG-dependent pathway.

Active ARF6 Promotes IP$_3$-induced Acrosomal Calcium Efflux during Sperm Exocytosis—Acrosomal exocytosis requires calcium release from internal stores, which is the final trigger for membrane fusion. The acrosome behaves as an internal store of releasable calcium (19, 47, 53, 54); efflux from this reservoir through IP$_3$-sensitive channels is required for the AR initiated by all inducers (22, 28, 33, 55). Results presented in Figs. 4*B*, 5, and 6 indicate that active ARF6 turns on the lipid branch. Fig. 6 suggests that the GTPase activates a PLC and consequently increases DAG and IP$_3$ (Fig. 7*A*). To assess whether calcium from an intracellular reservoir has a role in ARF6-induced AR, we used two unrelated specific IP$_3$-sensitive calcium channel inhibitors (2-APB and xestospongin C). Both inhibitors blocked myr-GTPγS-ARF6-induced secretion (Fig. 7*B*). Additionally, the membrane-permeant chelating agent that accumulates in the lumen of intracellular reservoirs, BAPTA-AM, abolished the acrosomal exocytosis induced by ARF6 (Fig. 7*B*). To summarize, these treatments significantly inhibited AR confirming that active ARF6-induced exocytosis requires calcium release from intracellular stores through IP$_3$-sensitive calcium channels and indirectly implies the involvement of a PLC downstream ARF6 in the signal transduction cascade.

We assumed that ARF6-induced AR inhibition secondary to blocking PLD activity or PIP$_2$ availability will occur due to lack of IP$_3$ synthesis. To test this argument, we resorted to the potent agonist of IP$_3$ receptors, adenophostin A. At the concentration tested, this reagent was not able to induce the AR by itself, but it rescued ARF6-induced exocytosis after PLD inhibition or PABD (Fig. 7*C*) and after sequestering PIP$_2$.[5] A corollary that emerges from this experiment is that IP$_3$ synthesis occurs downstream of ARF6.

We thus tested the prediction that myr-GTPγS-ARF6 activates the efflux of calcium from the acrosome in permeabilized cells. To directly assess this issue, acrosomes were loaded with the fluorescent calcium indicator Fluo3-AM, which accumulates in intracellular compartments in permeabilized cells. Calcium changes were measured in single cell experiments by fluorescence microscopy. Permeabilized cells showed staining at the acrosome region and midpiece (Fig. 8*A*), which is very different from the cytoplasmic distribution observed in nonpermeabilized spermatozoa (55). As shown in Fig. 8, *A–C*, and in supplemental Video 2, acrosomal fluorescence decreased immediately after active ARF6 addition. However, the midpiece staining remained unchanged. The spermatozoon midpiece contains mitochondria and was used as an internal control for photobleaching, because calcium from this source is not expected to be mobilized during secretion (Fig. 8, *A–C*). Taken together, these results lend support to the notion that active ARF6 leads to calcium efflux from the acrosome through IP$_3$-sensitive channels and that a PLC is activated during the process.

ARF6-induced Acrosome Reaction Requires Functional SNAREs— According to the two-branch hypothesis, ARF6 should activate

---

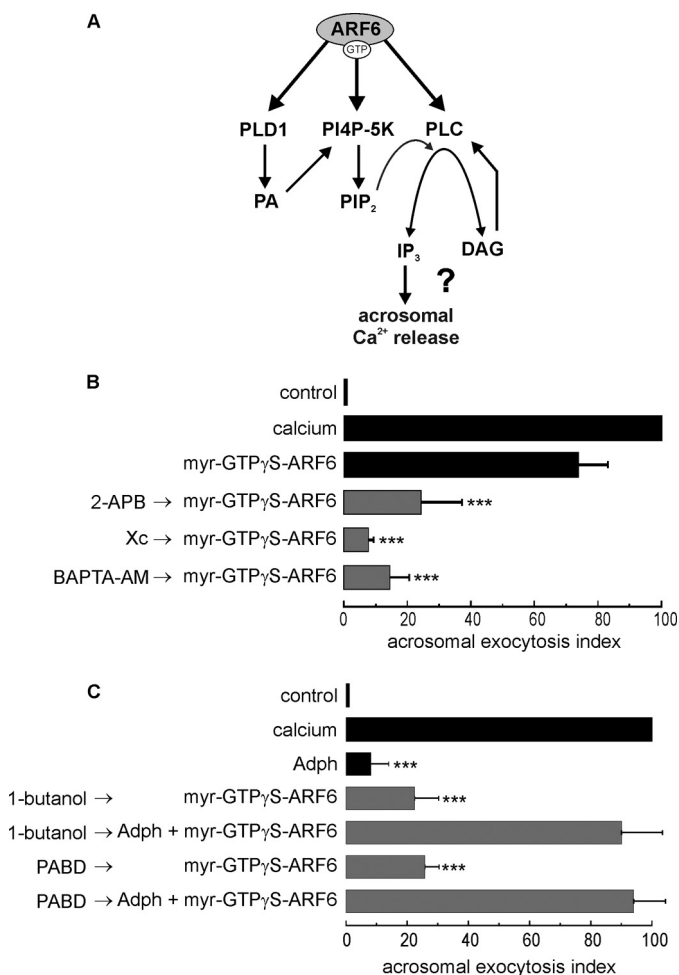[5] S. A. Belmonte, unpublished data.

FIGURE 7. **Active ARF6-induced exocytosis requires calcium release from intracellular stores through IP$_3$-sensitive calcium channels.** *A,* scheme depicting the hypothesis of ARF6-induced signaling pathway in acrosomal exocytosis. If ARF6 is activating PLC generating DAG and IP$_3$, then is IP$_3$ leading to calcium efflux from the acrosome? *B,* SLO-permeabilized sperm were treated with 100 μM 2-APB, 1.1 μM xestospongin C (*Xc*), or 10 μM BAPTA-AM for 15 min at 37 °C. Then cells were stimulated with 400 nM myr-GTPγS-ARF6. Several controls were included as follows: cells incubated at 37 °C for 15 min in HB-EGTA (*control*) or in HB-EGTA supplemented with 10 μM free calcium or 400 nM myr-GTPγS-ARF6. The data represent the mean $\pm$ S.E. from 5 to 10 independent experiments. Dunnett's test was used to compare the means of all groups against the calcium-stimulated condition and classified as not significant ($p > 0.05$) or significant (***, $p < 0.001$). *C,* adenophostin A, an agonist of IP$_3$ receptors, rescued ARF6-induced exocytosis after PLD inhibition. SLO-permeabilized human sperm were treated for 15 min with 0.5% 1-butanol or 10 μg/ml PABD. The samples were further incubated for 15 min with 400 nM myr-GTPγS-ARF6 supplemented, when indicated, with 2.5 μM adenophostin A (*1-butanol/PABD → adenophostin A + myr-GTPyS-ARF6*). Control conditions are shown as *black bars*; cells incubated in HB-EGTA (*control*), HB-EGTA with the addition of 10 μM of free calcium (*calcium*), or 2.5 μM adenophostin A (*Adph*). The data represent the mean $\pm$ S.E. from 5 to 10 independent experiments. Dunnett's test was used to compare the means of all groups against the calcium-stimulated condition and classified as not significant ($p > 0.05$) or significant (***, $p < 0.001$).

the protein branch, in addition to the lipid one, to induce exocytosis. In both intact and permeabilized sperm, calcium initiates a complex signaling cascade that culminates in the disassembly of neurotoxin-resistant *cis* and the assembly of toxin-sensitive loose *trans*-SNARE complexes required for exocytosis (22). We set out to evaluate whether ARF6-triggered exocytosis requires functional SNAREs (Fig. 9*A*). To assess this hypothesis, permeabilized sperm was incubated with the light chains of botulinum neurotoxin E (BoNT/E), C (BoNT/C), or TeTx

(BoNT/E cleaves SNAP25, BoNT/C cleaves syntaxin 1, and TeTx cleaves VAMP2) before ARF6 addition. All treatments abolished active ARF6-induced exocytosis (Fig. 9*B*). These results not only indicate that ARF6 acts by activating the fusion machinery, but they also rule out the possibility that recombinant ARF6 would be artifactually responsible for acrosome content release in human sperm due to membrane lipid alterations and membrane destabilization. We further evaluated the SNAP25 requirement for ARF6-induced exocytosis by adding anti-SNAP25 antibody before the ARF6 stimulus. The antibody blocked the ARF6-triggered exocytosis (Fig. 9*B*), presumably because it interfered with SNARE assembly in *trans*. Furthermore, we tested some other proteins implicated in acrosomal exocytosis. For instance, RIM is a cytosolic Rab3A effector that participates in acrosome-regulated exocytosis (56). We incubated permeabilized sperm with an anti-RIM1 antibody before adding active ARF6. The antibody inhibited ARF6-induced exocytosis (Fig. 9*B*), presumably because it interfered with the function of the endogenous protein. Roggero *et al.* (39) demonstrated that the C2B domain of synaptotagmin VI and an anti-complexin antibody blocked the formation of *trans*-SNARE complexes during the calcium-triggered AR in permeabilized human sperm. To further assess whether ARF6-induced exocytosis required the assembly of SNAREs in *trans*, we introduced the C2B domain of synaptotagmin VI or an anti-complexin antibody into permeabilized sperm before challenging with active ARF6. Evaluation of exocytosis of the acrosomes showed that both proteins inhibited exocytosis induced by the GTPase (Fig. 9*B*). Taken together, these results suggest that ARF6-elicited exocytosis needs functional SNAREs capable of forming *trans*-SNARE complexes to proceed, as well as some other proteins required for membrane fusion.

Active ARF6 Stimulates a GEF for Rab3A during Sperm Exocytosis—Rab3A has been characterized as one of the earliest factors in the protein branch cascade during sperm exocytosis (25, 26). To determine whether Rab3A is involved in ARF6-evoked secretion (Fig. 10*A*), we introduced anti-Rab3A antibodies in SLO-permeabilized sperm before challenging with active ARF6. The antibody inhibited ARF6-induced exocytosis, indicating that Rab3A is part of the mechanism stimulated by ARF6 (Fig. 10*B*). If GTP-bound Rab3A is required for ARF6-induced AR, we should be able to inhibit exocytosis by sequestering active Rab3A with the Rab3-GTP binding domain of RIM (RIM-RBD, amino acids 11–398) (57). This domain inhibited the ARF6-induced AR (Fig. 10*B*). These results suggest that Rab3A activation is necessary for ARF6-elicited exocytosis. Does ARF6 activate Rab3A? We conducted pulldown assays to answer this question. Permeabilized cells were loaded with geranylgeranylated recombinant Rab3A-GDP before challenging with active ARF6. Subsequently, we conducted pulldown assays using the Rab3-GTP binding domain of RIM mentioned above. As shown in Fig. 10*C*, the Rab3A-GTP levels increased 2-fold (quantification in Fig. 10*D*) upon treatment with ARF6, suggesting that human sperm contains an activity that exchanges GDP for GTP in Rab3A in response to ARF6. DAG was used as a positive control as we have previously shown that it promotes Rab3A GDP/GTP exchange (33). We used sperm
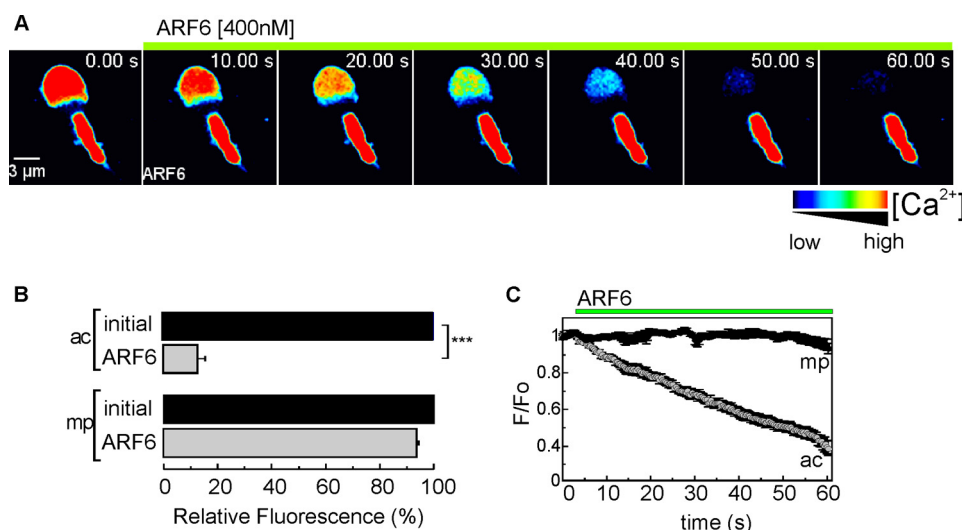
FIGURE 8. **Active ARF6 promotes IP$_3$-induced acrosomal calcium efflux during sperm exocytosis.** *A,* SLO-permeabilized sperm were incubated with 100 nM BoNT/C and 2 μM Fluo3-AM for 30 min at 37 °C. The fluorescence was recorded in an inverted microscope. Representative images of Fluo3-AM-loaded human sperm before and after the treatment with 400 nM myr-GTPγS-ARF6. Images are shown in pseudocolor (*blue* and *red* represent low and high [Ca^{2+}]$_i$, respectively). *B,* relative fluorescence comparing initial values (100%) and 50 s after 400 nM myr-GTPγS-ARF6 stimulation in the acrosomal and midpiece regions. *Bars* represent the mean $\pm$ S.E. ($n = 15$). *Asterisks* indicate significant difference (***, $p < 0.001$) from the initial value (single group analysis, 99.9% confidence interval). *C,* plot illustrates the traces corresponding to *B* for the acrosomal (*ac*) and midpiece (*mp*) regions. The scales indicate (F/F_o) *versus* time (s).
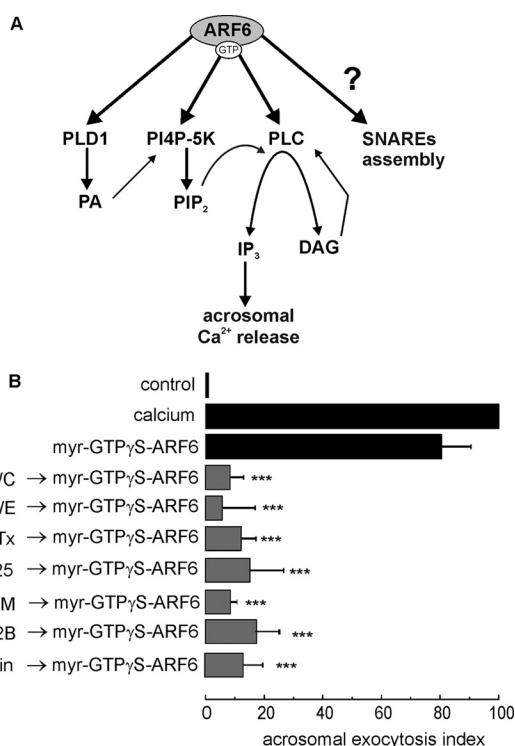

FIGURE 9. **ARF6-induced acrosome reaction requires functional SNAREs.** *A,* scheme depicting the hypothesis of ARF6-induced signaling pathway in acrosomal exocytosis. Does ARF6 require SNARE assembly to induce AR? *B,* permeabilized human sperm cells were incubated with compounds affecting SNAREs availability: 100 nM BoNT/C (light chain), to cleave syntaxin1; 300 nM BoNT/E (light chain), to cleave SNAP25; 100 nM TeTx (light chain), to cleave VAMP2; 10 μg/ml anti-RIM antibody, 20 μg/ml anti-SNAP25 antibody, 500 nM C2B domain of synaptotagmin, or 70 nM anti-complexin antibody for 15 min at 37 °C. Acrosome reaction was then stimulated with 400 nM myr-GTPγS-ARF6 for a further 15 min at 37 °C. Several controls were included: background acrosome reaction in the absence of any stimulation (control), 400 nM myr-GTPγS-ARF6, or 0.5 mM CaCl$_2$ (10 μM free calcium). The data represent the mean $\pm$ S.E. of at least five independent experiments. Dunnett's test was used to compare the means of all groups against the calcium-stimulated condition in the absence of inhibitors and classified as not significant ($p > 0.05$) or significant differences (***, $p < 0.001$).

tubulin, present in the unbound fraction of the pulldown assay, as loading control (Fig. 10*E*).

We were interested in determining the percentage of the sperm population that exhibits endogenous, active Rab3 in response to ARF6 treatment and where in the cells Rab3-GTP localizes. To this end, we used the protocol described and validated by Bustos *et al.* (38). The protocol is based on the principles underlining far-Western blot analysis, but with indirect immunofluorescence as the readout. Permeabilized sperm were incubated with different exocytic stimuli as follows: calcium, DAG, or active ARF6 except in the control condition. To quantify the activation state of Rab3, we overlaid fixed cells with GST-RIM-RBD. We detected the activation probe by standard immunostaining using anti-GST antibodies. As shown in Fig. 10*F*, Rab3-GTP localized to the acrosomal region. By subtracting the percentage of cells immunostained under control conditions, we observed an increase of 20–25% of cells decorated when treated with calcium or active ARF6 and ~35% of the cells treated with DAG (Fig. 10, *F* and *G*). Our results indicate that ARF6-GTP activates a GEF for Rab3A increasing the level of endogenous Rab3A-GTP during sperm exocytosis, thus putting into motion the protein limb of the signaling cascade.

Effects of AR Inducers on ARF6 Activation Status, Calcium and DAG Stimulate a GEF for ARF6 during Sperm Exocytosis— Having established that ARF6 is present in human sperm and that bacterially expressed, lipid-modified, and GTP-bound ARF6 activates PLD, PI4P-5K, PLC, and Rab3A during the AR, we asked whether the onset of exocytosis also activates ARF6 (Fig. 11*A*). We measured the activation state of ARF6 using the GGA-GAT pulldown assay described in Cohen *et al.* (58). We used the VHS-GAT domain of the GGA protein (for Golgi localizing adaptin ear homology domain ARF-binding protein). This domain specifically recognizes the GTP-bound form of ARF but does not bind to the GDP-bound form. Nevertheless, we ran specificity controls for this domain in a pulldown assay
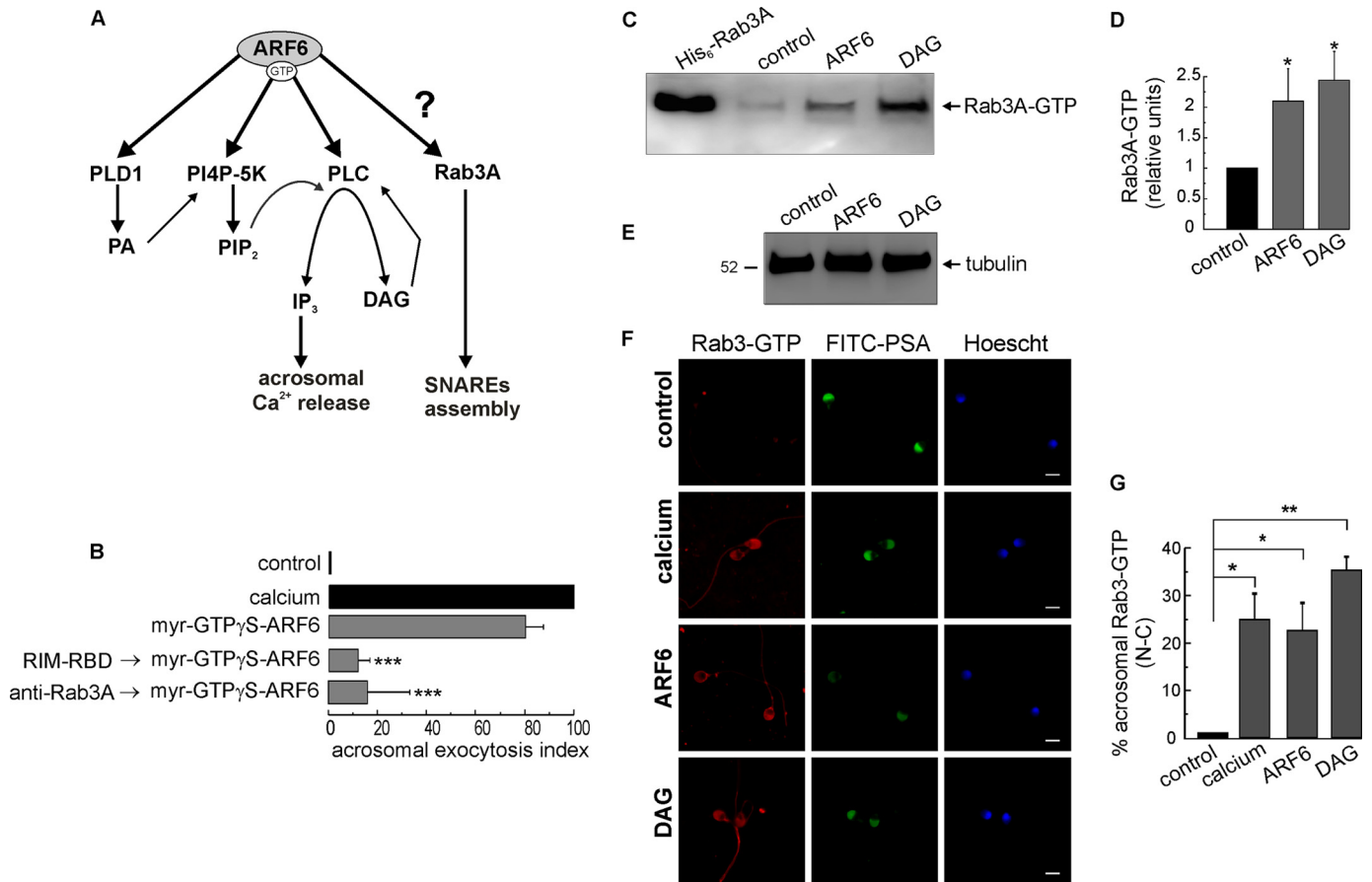
FIGURE 10. **Active ARF6 stimulates a GEF for a Rab3A during sperm exocytosis.** *A,* scheme depicting the hypothesis of ARF6-induced signaling pathway in acrosomal exocytosis. Does ARF6 require Rab3A-GTP to induce AR? Is ARF6 able to activate a GEF for Rab3A? *B,* SLO-permeabilized human sperm were treated for 15 min at 37 °C with 10 μg/ml anti-Rab3A antibodies or 5 μg/ml RIM-RBD. The samples were further incubated for 15 min at 37 °C with 400 nM myr-GTPγS-ARF6. Control conditions are shown as *black bars*: AR in the absence of any stimulation (*control*), incubated in the presence of 10 μM free calcium, or 400 nM myr-GTPγS-ARF6. The data represent the mean $\pm$ S.E. from 5 to 10 independent experiments. Dunnett's test was used to compare the means of all groups against the calcium-stimulated condition in the absence of inhibitors and classified as not significant ($p > 0.05$) or significant (***, $p < 0.001$). *C,* 30 $\times$ 10^6 permeabilized sperm were incubated for 15 min at 37 °C with 100 μM 2-APB, loaded with 10 nM His$_6$-Rab3A-GDP, and either not treated further (*control*) or incubated with 10 μM DAG or 400 nM myr-GTPγS-ARF6 for 15 min at 37 °C. Whole cell lysates were subjected to pull down assays using RIM-RBD-Sepharose beads, and the levels of Rab3A-GTP were analyzed by Western blot. Recombinant Rab3A was used as a control (*His$_6$-Rab3A*). *D,* quantification of the immuno-blot (ImageJ). The *graph* represents the mean $\pm$ S.E. from all replicates; * significantly different from 1, *t* test for single group mean. A blot representative of three repetitions is shown. *E,* anti-α-tubulin was used as an input control. *F,* SLO-permeabilized sperm were incubated with 2-APB for 10 min at 37 °C. They were then treated with 10 μM free calcium, 400 nM myr-GTPγS-ARF6, or 10 μM DAG for 15 min at 37 °C. Cells were triple-stained with an anti-GST antibody as a readout for the activity probes that detect active Rab3 (*red*), with FITC-PSA, to evaluate the acrosome status (*green*), and with Hoechst 33342 to visualize all cells in the field (*blue*). *Scale bars,* 5 μm. *G,* quantifications (mean $\pm$ S.E. of at least three independent experiments) are shown to the *right*. Significant differences (**, $p < 0.01$; *, $p < 0.05$) are indicated for each bar. Differences were considered not significant at $p < 0.05$.

and confirmed that it binds only to the GTP form. In brief, we incubated glutathione-Sepharose beads containing VHS-GAT expressed as a GST fusion protein with myristoylated His$_6$-myr-GDPβS-ARF6 or His$_6$-myr-GTPγS-ARF6. Bound proteins were analyzed by Western blot using a specific anti-ARF6 antibody. The domain pulled down ARF6-GTPγS but not ARF6-GDPβS, demonstrating the domain specificity (Fig. 11*B*).

We then applied this pulldown strategy to examine the effects of AR inducers on the GTP status of ARF6. We loaded permeabilized sperm with myristoylated His$_6$-ARF6-GDP followed by exocytic stimuli (calcium or PMA). We replaced DAG with PMA, an analogue that has the same effects as DAG on the AR (33). VHS-GAT immobilized on glutathione-Sepharose beads was incubated with lysates from sperm incubated under the conditions mentioned above. The ARF6-GTP levels increased ~2-fold upon stimulation with calcium or PMA (Fig. 11, *C* and *D*). These results suggest that human sperm are capable of exchanging GDP for GTP on ARF6

and that this activity increases in response to both exocytic stimuli. We used sperm tubulin, present in the unbound fraction of the pulldown assay, as loading control (Fig. 11*E*). In conclusion, both exocytic stimuli, calcium and DAG, activate a GEF for ARF6 through a still undefined mechanism.

DISCUSSION

ARF6 plays pivotal roles in a wide variety of cellular events, including exocytosis, endocytosis, actin cytoskeleton reorganization, and phosphoinositide metabolism, in various types of cells (2, 59–61). Evidence suggesting its implication in exocytosis comes mostly from studies in neurons and endocrine and neuroendocrine cells, (3, 13, 62, 63). The downstream effector(s) of ARF6 in exocytosis remain uncertain, although linked to the regulation of lipid synthesis. The positive effects of active ARF6 on exocytosis were attributed to PIP$_2$ and PA synthesis in different secretory cell models (11, 17, 64–66). Previous studies
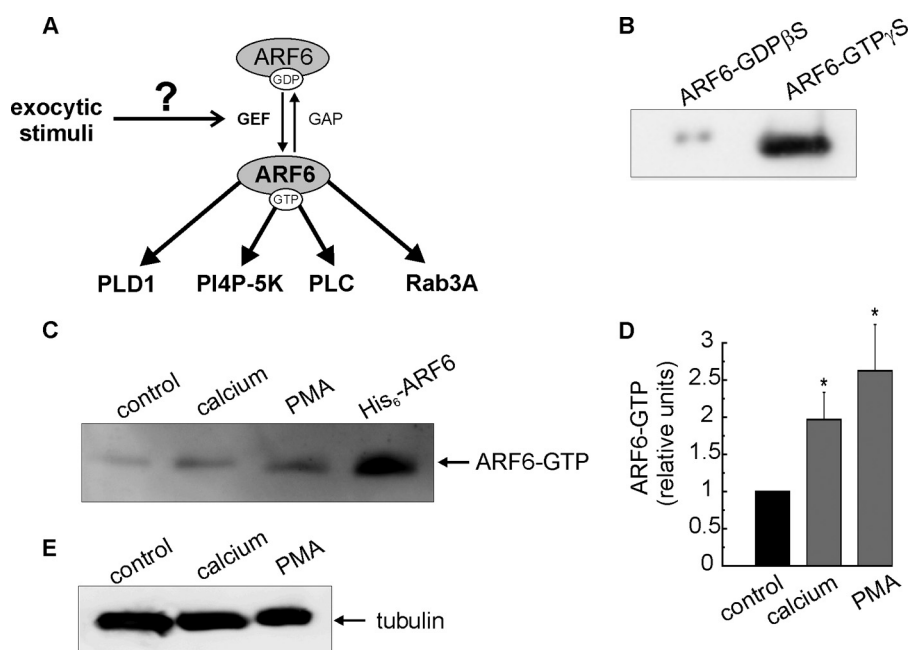
FIGURE 11. **Calcium and DAG stimulate a GEF for ARF6 during sperm exocytosis.** *A*, are exocytic stimuli able to activate a GEF for ARF6? *B*, recombinant ARF6 proteins (100 nM myr-GTPγS-ARF6 or 100 nM myr-GDPβS-ARF6) were pulled down with the VHS-GAT-Sepharose beads. The levels of ARF6 bound to the beads were analyzed by Western blot. *C*, SLO-permeabilized human sperm (30×10^6 cells) were incubated for 15 min at 37 °C with 100 μM 2-APB. Cells were then loaded with 10 nM myr-ARF6-GDP for 15 min and were incubated or not (*control*) with 10 μM calcium or 200 nM PMA for 15 min at 37 °C. Whole cell lysates were subjected to pulldown assays using VHS-GAT-Sepharose beads, and the levels of ARF6 bound to GTP were analyzed by Western blot. Recombinant ARF6 used for the pulldown assay was used as a control (*His₆-ARF6*). A blot representative of three repetitions is shown. *D*, quantification of the immunoblot (ImageJ) is represented as mean ± S.E. from all replicates; * significantly different from 1, *t* test for single group mean. *E*, anti-α-tubulin was used as an input control.

describing the function of ARF6 on secretion have employed cells capable of undergoing all the membrane traffic processes involving ARF6; therefore, they cannot isolate the molecular mechanism by which the GTPase specifically regulates exocytosis. Here, we use human spermatozoa, a cell lacking all membrane traffic phenomena except exocytosis, to provide insights into this issue. While scrutinizing the literature for information on ARF6 in sperm, we found a report demonstrating its presence in the male reproductive tract in *Drosophila*, where the GTPase is required for spermatocyte cytokinesis (67). Moreover, Baker *et al.* (68) characterized the mouse sperm proteome and identified the presence of ARF6 in the gametes.

A central challenge in the field of reproduction is to understand how sperm regulate the secretion machinery to release its acrosomal content only when it finds the egg. Understanding how lipid concentrations are modified when exocytic stimuli are applied is a major issue in cell and reproductive biology. Recently, we described that DAG stimulates acrosomal exocytosis in permeabilized sperm by feeding into a PLD-dependent positive-feedback loop that continuously supplies PIP₂ (33). Given that ARF6 is known to regulate PIP₂ and PA concentrations, both essential for acrosomal exocytosis, we focused on the role of this small GTPase on the release of the human sperm secretory granule contents. Here, we revealed the presence of ARF6 in human sperm and demonstrated for the first time its requirement in sperm-regulated secretion.

We report in this paper that myristoylated and GTP-loaded ARF6 added to permeabilized cells induces acrosomal exocytosis in a dose-dependent fashion and in the absence of extracellular calcium. Because these findings were somewhat unexpected, we confirmed them by assessing exocytosis with three different methods as follows: (i) the classic or indirect staining, by adding FITC-PSA after fixation; (ii) direct staining, by including FITC-PSA in the incubation medium before stimulus addition and fixation; and (iii) using both flow cytometry and confocal microscopy in real time experiments (without fixation). All three methods gave similar results. These methods provide new trustworthy tools to evaluate exocytosis in permeabilized sperm.

In agreement with the observations that ARF6 modulates exocytosis through PIP₂ and PA synthesis, sperm secretion experiments defined the requirement for PLD1 in ARF6-induced exocytosis. We established that ARF6 induces PIP₂ synthesis, suggesting the participation of a PI4P-5K during the exocytic process. Both results indicate that the small GTPase is modifying membrane lipids, as described in other systems. Nonetheless, we recently reported that, despite the fact that both phospholipids are absolutely required for sperm AR, neither PA nor PIP₂ is able to trigger exocytosis alone (33). Exocytosis of the acrosome is a multistage process involving the opening of ion channels, activation of multiple signaling pathways, and orchestration of numerous protein-protein interactions to finally put the fusion machinery in place and produce calcium efflux from the acrosome through IP₃-sensitive channels. It would appear that the generation of PIP₂ and PA due to active ARF6 is not in itself enough to accomplish exocytosis. Next, we set out to uncover the molecular mechanism whereby ARF6 produces exocytosis.

In evaluating whether ARF6 affected both pivotal limbs required for acrosomal exocytosis to proceed (27, 28), we found that ARF6 stimulated a PLC activity and that this effect was required to induce regulated secretion. We emphasize the importance of the semiquantitative assay we developed to

determine PLC activity. The assays used to assess PLC activity mostly utilize $[^3H]PIP_2$ and measurement of the hydrolysis product, IP_3 (method modified from Ref. 69). This method was used in sperm (70), eggs (71), tsA-201 cells (human embryonic kidney) (72), etc. Other methods currently in use are indirect, given that they evaluate calcium oscillations/concentration (73, 74) to infer PLC activity. Our method allowed us to determine that PIP_2 hydrolysis, induced by ARF6, decreased when DAG was sequestered by the C1 domain of Munc13-1. This result suggests that GTP-bound ARF6 promotes PLC activity, and the production of DAG reinforces the effect.

We propose PLCϵ as a candidate for the effect caused by ARF6, given that it is unique in relation to other PLC isoforms in terms of its ability to be regulated by multiple signaling inputs. Mammalian PLCϵ contains two Ras/Rap1-associating domains and a CDC25 homology domain that exhibits *in vitro* GEF activity toward Rap1. The RA2 domain of PLCϵ associates with GTP-bound Rap1A, suggesting that PLCϵ is regulated downstream of these small GTPases. The CDC25 homology domain may stimulate the formation of Rap1-GTP (75) generating a positive feedback loop. Previously, it has been reported that cAMP elicits acrosomal exocytosis via Epac, a GEF for Rap1 (28, 76). We published recently that DAG-induced exocytosis required the small GTPase Rap1 to proceed (33), and we proposed a requirement for a DAG-sensitive GEF for Rap1 (RapGRP/CalDAG (77)) to activate PLCϵ, providing a second positive feedback loop. ARF6, which also belongs to the Ras family, may directly activate PLCϵ (75). The evidence presented here leads us to posit that the ARF6 effect is reinforced by DAG production. In summary, we demonstrate that ARF6 is able to activate a phosphoinositide-specific PLC during exocytosis. This finding implies that it regulates IP_3-dependent calcium release from intracellular stores and the DAG cascades.

To evaluate the downstream effects of PLC activation by ARF6, we manipulated IP_3 function demonstrating indirectly the participation of a PLC downstream-active ARF6. Most importantly, we directly demonstrated by single cell, real time fluorescence microscopy that ARF6 induces the efflux of calcium from the acrosome in permeabilized cells. Our experimental data in sperm cells provide strong evidence for cleavage of PIP_2 by PLC induced by active ARF6.

According to previous results, acrosome secretion requires not only the release of calcium from intracellular stores but also the activation of a complex membrane fusion machinery, including Rab3A, NSF, SNAREs, complexin, and synaptotagmin (78). To trigger exocytosis, ARF6 should, in addition to producing IP_3, activate this machinery. Here, we showed that ARF6-induced exocytosis requires active Rab3A to proceed, and by using pulldown assays, we demonstrated that the small GTPase stimulated the accumulation of Rab3A in the active form in sperm, suggesting the activation of a GEF for Rab3A during exocytosis. Our experiments were aimed at determining whether ARF6 stimulates GDP/GTP exchange in Rab3A. Rab3-GAP1 and -2 were detected in a murine haploid germ cell proteome (79) and in the human sperm proteome. In the last one, a GEF for Rab3A was found too (80).

Pulldown assays report the activation status of the recombinant Rab added to the system and do not provide information about the location of the active protein. A far immunofluores-cence assay allowed us to report an increased number of cells evincing endogenous GTP-bound Rab3 in the acrosomal region in response to active ARF6. These results reinforce the idea that ARF6 acts upstream of Rab3A during the exocytotic cascade leading to acrosomal release. GTPases work cooperatively on the same traffic pathway and are coordinately regulated to accomplish their functions in a sequential fashion (81). One of the most studied regulatory mechanisms has been termed the Rab GEF cascade and proposes that an upstream active Rab recruits the GEF for the Rab acting immediately downstream, thereby initiating Rab conversion along the pathway. It has been described that ARF6 networks with Rab proteins through cascade mechanisms (81). We show here that the molecular mechanism that governs the activation of Rab3 by ARF6 may act through a Rab GEF cascade. By using a combination of neurotoxins, antibodies, and domains of different proteins involved in membrane fusion, we demonstrated that ARF6-elicited exocytosis needs functional SNAREs capable of forming *trans*-SNARE complexes, as well as complexin, synaptotagmin, and RIM. Together, the induction of the AR with active ARF6 results in Rab3A activation and SNARE assembly.

In this study, by means of pulldown we showed that both calcium and PMA induce a significant increase in ARF6-GTP levels. Therefore, we report here that sperm contain a GEF activity that exchanges GDP for GTP on ARF6 when challenged with exocytic stimuli. A fundamental but yet unresolved issue in cell biology is how GEFs for ARF6 are regulated. Eight proteins, classified in three GEF families (cytohesin, EFA6, and BRAG), were shown to act on ARF6 (82). All ARF6 GEFs possess a pleckstrin homology domain that serves as a binding site for specific phosphoinositides and/or partner proteins. They are recruited to the membranes through an interaction with PIP_2 or PIP_3, depending on the different affinities of pleckstrin homology domains for these phospholipids (83, 84). The synthesis of PIP_2 and/or PIP_3 may be one of the major mechanisms through which ARF6 is activated at the membrane in response to agonist stimulation of cells (85).

Suzuki *et al.* (86) reported the presence of an ARF6-GEF in the male reproductive tract demonstrating that EFA6 is localized in spermatogenic cells of adult mice testes. Baker *et al.* (87) characterized the human sperm proteome and identified the presence of an ARF6 GAP of the BRAG family in male gametes. Recently, in-depth proteomic analysis of the human sperm revealed that ARF1, -4, -5, and -6 are present in the male gamete as well as different GAPs and GEFs for these GTPases (ACAP2, GIT1, AGAP1 and -3, ARF, GEF1 and -2) (80). The presence and function of these ARF6-GEFs have been extensively described in secretory cells, *e.g.* chromaffin cells (12) and neurons (88, 89). Given that diverse exocytic stimuli induce changes in the sperm lipid profile (90, 91), and in particular that PIP_2 (33) and PIP_3 levels (92) are increased, we hypothesize that both lipids contribute to ARF6-GEs binding to membranes, triggering ARF6 activation and the signal transduction cascade described. Further studies are needed, however, to assess the presence of GEFs and GAPs for ARF6 in human spermatozoa.

On the basis of the results presented here, we built a working model depicting our current thinking on the mechanisms underlying acrosomal exocytosis (Fig. 12). In permeabilized
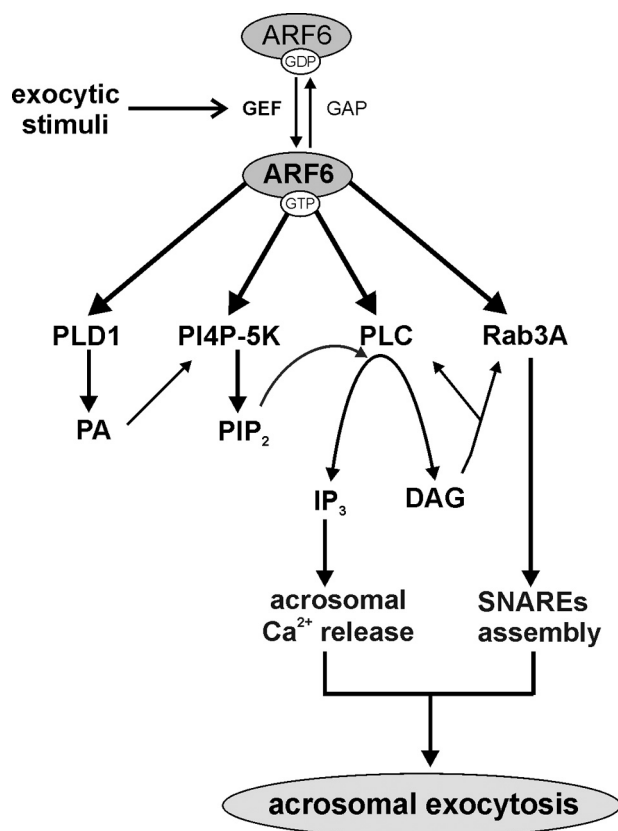
FIGURE 12. **Working model of the signaling cascade triggered by ARF6 during acrosomal exocytosis.** In permeabilized human sperm, ARF6 once activated by exocytic stimuli stimulates PLD1, PI4P-5K, and PLC activities driving PIP_2 turnover and IP_3 synthesis with the consequent mobilization of calcium from an intracellular store. However, Rab3A is activated leading to the assembly of the membrane fusion machinery. Both calcium efflux from the acrosome and SNAREs assembly lead to acrosomal exocytosis.

human sperm ARF6, once activated, stimulates PLD1, PI4P-5K, and PLC activities, driving PIP_2 turnover and IP_3 synthesis, with the consequent mobilization of calcium from an intracellular store. Concomitantly, the GTPase activates Rab3A that leads to the assembly of the fusion protein machinery, allowing the outer acrosomal and plasma membranes to become physically attached. The results described here show that active ARF6 induces endogenous Rab3A GDP/GTP exchange and fosters phospholipid remodeling for the continuous production and hydrolysis of PIP_2 and IP_3 release. Here, we propose a role for this multitasking GTPase in sperm acrosome reaction and demonstrate its activation by exocytic stimuli. The functional and biochemical characterization of ARF6 regulation of acrosomal exocytosis reported in our study may provide some clues as to how secretion could be modulated in other exocytic cells.

REFERENCES

1. Randazzo, P. A., Nie, Z., Miura, K., and Hsu, V. W. (2000) Molecular aspects of the cellular activities of ADP-ribosylation factors. *Sci. Signal. STKE 2000/59/re1*
2. D'Souza-Schorey, C., and Chavrier, P. (2006) ARF proteins: roles in membrane traffic and beyond. *Nat. Rev. Mol. Cell Biol.* **7,** 347–358
3. Donaldson, J. G. (2003) Multiple roles for Arf6: sorting, structuring, and signaling at the plasma membrane. *J. Biol. Chem.* **278,** 41573–41576
4. Schafer, D. A., D'Souza-Schorey, C., and Cooper, J. A. (2000) Actin assembly at membranes controlled by ARF6. *Traffic* **1,** 892–903
5. Powelka, A. M., and Buckley, K. M. (2001) Expression of ARF6 mutants in neuroendocrine cells suggests a role for ARF6 in synaptic vesicle biogenesis. *FEBS Lett.* **501,** 47–50
6. Lawrence, J. T., and Birnbaum, M. J. (2003) ADP-ribosylation factor 6 regulates insulin secretion through plasma membrane phosphatidylinositol 4,5-bisphosphate. *Proc. Natl. Acad. Sci. U.S.A.* **100,** 13320–13325
7. Burgoyne, R. D., and Morgan, A. (2003) Secretory granule exocytosis. *Physiol. Rev.* **83,** 581–632
8. Caumont, A. S., Galas, M. C., Vitale, N., Aunis, D., and Bader, M. F. (1998) Regulated exocytosis in chromaffin cells. Translocation of ARF6 stimulates a plasma membrane-associated phospholipase D. *J. Biol. Chem.* **273,** 1373–1379
9. Galas, M. C., Helms, J. B., Vitale, N., Thiersé, D., Aunis, D., and Bader, M. F. (1997) Regulated exocytosis in chromaffin cells. A potential role for a secretory granule-associated ARF6 protein. *J. Biol. Chem.* **272,** 2788–2793
10. Vitale, N., Chasserot-Golaz, S., Bailly, Y., Morinaga, N., Frohman, M. A., and Bader, M. F. (2002) Calcium-regulated exocytosis of dense-core vesicles requires the activation of ADP-ribosylation factor (ARF)6 by ARF nucleotide binding site opener at the plasma membrane. *J. Cell Biol.* **159,** 79–89
11. Béglé, A., Tryoen-Tóth, P., de Barry, J., Bader, M. F., and Vitale, N. (2009) ARF6 regulates the synthesis of fusogenic lipids for calcium-regulated exocytosis in neuroendocrine cells. *J. Biol. Chem.* **284,** 4836–4845
12. Caumont, A. S., Vitale, N., Gensse, M., Galas, M. C., Casanova, J. E., and Bader, M. F. (2000) Identification of a plasma membrane-associated guanine nucleotide exchange factor for ARF6 in chromaffin cells. Possible role in the regulated exocytotic pathway. *J. Biol. Chem.* **275,** 15637–15644
13. Zheng, Q., and Bobich, J. A. (2004) ADP-ribosylation factor6 regulates both [³H]noradrenaline and [¹⁴C]glutamate exocytosis through phosphatidylinositol 4,5-bisphosphate. *Neurochem. Int.* **45,** 633–640
14. Bader, M. F., and Vitale, N. (2009) Phospholipase D in calcium-regulated exocytosis: lessons from chromaffin cells. *Biochim. Biophys. Acta* **1791,** 936–941
15. Honda, A., Nogami, M., Yokozeki, T., Yamazaki, M., Nakamura, H., Watanabe, H., Kawamoto, K., Nakayama, K., Morris, A. J., Frohman, M. A., and Kanaho, Y. (1999) Phosphatidylinositol 4-phosphate 5-kinase α is a downstream effector of the small G protein ARF6 in membrane ruffle formation. *Cell* **99,** 521–532
16. Massenburg, D., Han, J. S., Liyanage, M., Patton, W. A., Rhee, S. G., Moss, J., and Vaughan, M. (1994) Activation of rat brain phospholipase D by ADP-ribosylation factors 1, 5, and 6: separation of ADP-ribosylation factor-dependent and oleate-dependent enzymes. *Proc. Natl. Acad. Sci. U.S.A.* **91,** 11718–11722
17. Vitale, N. (2010) Synthesis of fusogenic lipids through activation of phospholipase D1 by GTPases and the kinase RSK2 is required for calcium-regulated exocytosis in neuroendocrine cells. *Biochem. Soc. Trans.* **38,** 167–171
18. Yanagimachi, R. (1994) in *The Physiology of Reproduction* (Knobil, E. N., and Neill, J., eds) pp. 189–317, Raven Press, New York
19. Costello, S., Michelangeli, F., Nash, K., Lefievre, L., Morris, J., Machado-Oliveira, G., Barratt, C., Kirkman-Brown, J., and Publicover, S. (2009) Ca²⁺-stores in sperm: their identities and functions. *Reproduction* **138,** 425–437
20. Darszon, A., Acevedo, J. J., Galindo, B. E., Hernández-González, E. O., Nishigaki, T., Treviño, C. L., Wood, C., and Beltrán, C. (2006) Sperm channel diversity and functional multiplicity. *Reproduction* **131,** 977–988

21. Tomes, C. N., Michaut, M., De Blas, G., Visconti, P., Matti, U., and Mayorga, L. S. (2002) SNARE complex assembly is required for human sperm acrosome reaction. *Dev. Biol.* **243**, 326–338

22. De Blas, G. A., Roggero, C. M., Tomes, C. N., and Mayorga, L. S. (2005) Dynamics of SNARE assembly and disassembly during sperm acrosomal exocytosis. *PLoS Biol.* **10**, e323

23. Tomes, C. N., De Blas, G. A., Michaut, M. A., Farré, E. V., Cherhitin, O., Visconti, P. E., and Mayorga, L. S. (2005) α-SNAP and NSF are required in a priming step during the human sperm acrosome reaction. *Mol. Hum. Reprod.* **11**, 43–51

24. Roggero, C. M., Tomes, C. N., De Blas, G. A., Castillo, J., Michaut, M. A., Fukuda, M., and Mayorga, L. S. (2005) Protein kinase C-mediated phosphorylation of the two polybasic regions of synaptotagmin VI regulates their function in acrosomal exocytosis. *Dev. Biol.* **285**, 422–435

25. Yunes, R., Michaut, M., Tomes, C., and Mayorga, L. S. (2000) Rab3A triggers the acrosome reaction in permeabilized human spermatozoa. *Biol. Reprod.* **62**, 1084–1089

26. Lopez, C. I., Belmonte, S. A., De Blas, G. A., and Mayorga, L. S. (2007) Membrane-permeant Rab3A triggers acrosomal exocytosis in living human sperm. *FASEB J.* **21**, 4121–4130

27. Branham, M. T., Mayorga, L. S., and Tomes, C. N. (2006) Calcium-induced acrosomal exocytosis requires cAMP acting through a protein kinase A-independent, Epac-mediated pathway. *J. Biol. Chem.* **281**, 8656–8666

28. Branham, M. T., Bustos, M. A., De Blas, G. A., Rehmann, H., Zarelli, V. E., Treviño, C. L., Darszon, A., Mayorga, L. S., and Tomes, C. N. (2009) Epac activates the small G proteins Rap1 and Rab3A to achieve exocytosis. *J. Biol. Chem.* **284**, 24825–24839

29. Hafez, I., Stolpe, A., and Lindau, M. (2003) Compound exocytosis and cumulative fusion in eosinophils. *J. Biol. Chem.* **278**, 44921–44928

30. Zheng, Q., Bobich, J. A., Vidugiriene, J., McFadden, S. C., Thomas, F., Roder, J., and Jeromin, A. (2005) Neuronal calcium sensor-1 facilitates neuronal exocytosis through phosphatidylinositol 4-kinase. *J. Neurochem.* **92**, 442–451

31. Díaz, A., Domínguez, L., Fornés, M. W., Burgos, M. H., and Mayorga, L. S. (1996) Acrosome content release in streptolysin O permeabilized mouse spermatozoa. *Andrologia* **28**, 21–26

32. Ackermann, F., Zitranski, N., Borth, H., Buech, T., Gudermann, T., and Boekhoff, I. (2009) CaMKIIα interacts with multi-PDZ domain protein MUPP1 in spermatozoa and prevents spontaneous acrosomal exocytosis. *J. Cell Sci.* **122**, 4547–4557

33. Lopez, C. I., Pelletán, L. E., Suhaiman, L., De Blas, G. A., Vitale, N., Mayorga, L. S., and Belmonte, S. A. (2012) Diacylglycerol stimulates acrosomal exocytosis by feeding into a PKC- and PLD1-dependent positive loop that continuously supplies phosphatidylinositol 4,5-bisphosphate. *Biochim. Biophys. Acta* **1821**, 1186–1199

34. Belmonte, S. A., López, C. I., Roggero, C. M., De Blas, G. A., Tomes, C. N., and Mayorga, L. S. (2005) Cholesterol content regulates acrosomal exocytosis by enhancing Rab3A plasma membrane association. *Dev. Biol.* **285**, 393–408

35. Tomes, C. N. (2007) Molecular mechanisms of membrane fusion during acrosomal exocytosis. *Soc. Reprod. Fertil. Suppl.* **65**, 275–291

36. Kassas, N., Tryoen-Tóth, P., Corrotte, M., Thahouly, T., Bader, M. F., Grant, N. J., and Vitale, N. (2012) Genetically encoded probes for phosphatidic acid. *Methods Cell Biol.* **108**, 445–459

37. Wang, L., Li, G., and Sugita, S. (2005) A central kinase domain of type I phosphatidylinositol phosphate kinases is sufficient to prime exocytosis: isoform specificity and its underlying mechanism. *J. Biol. Chem.* **280**, 16522–16527

38. Bustos, M. A., Lucchesi, O., Ruete, M. C., Mayorga, L. S., and Tomes, C. N. (2012) Rab27 and Rab3 sequentially regulate human sperm dense-core granule exocytosis. *Proc. Natl. Acad. Sci. U.S.A.* **109**, E2057–E2066

39. Roggero, C. M., De Blas, G. A., Dai, H., Tomes, C. N., Rizo, J., and Mayorga, L. S. (2007) Complexin/synaptotagmin interplay controls acrosomal exocytosis. *J. Biol. Chem.* **282**, 26335–26343

40. Klein, S., Franco, M., Chardin, P., and Luton, F. (2006) Role of the Arf6 GDP/GTP cycle and Arf6 GTPase-activating proteins in actin remodeling and intracellular transport. *J. Biol. Chem.* **281**, 12352–12361

41. Schägger, H., and von Jagow, G. (1987) Tricine-sodium dodecyl sulfate-polyacrylamide gel electrophoresis for the separation of proteins in the range from 1 to 100 kDa. *Anal. Biochem.* **166**, 368–379

42. Belmonte, S. A., and Suhaiman, L. (2012) Optimized protocols to analyze sphingosine-1-phosphate signal transduction pathways during acrosomal exocytosis in human sperm. *Methods Mol. Biol.* **874**, 99–128

43. Schweitzer, J. K., and D'Souza-Schorey, C. (2002) Localization and activation of the ARF6 GTPase during cleavage furrow ingression and cytokinesis. *J. Biol. Chem.* **277**, 27210–27216

44. Cross, N. L., and Meizel, S. (1989) Methods for evaluating the acrosomal status of mammalian sperm. *Biol. Reprod.* **41**, 635–641

45. Mendoza, C., Carreras, A., Moos, J., and Tesarik, J. (1992) Distinction between true acrosome reaction and degenerative acrosome loss by a one-step staining method using *Pisum sativum* agglutinin. *J. Reprod. Fertil.* **95**, 755–763

46. Zoppino, F. C., Halón, N. D., Bustos, M. A., Pavarotti, M. A., and Mayorga, L. S. (2012) Recording and sorting live human sperm undergoing acrosome reaction. *Fertil. Steril.* **97**, 1309–1315

47. De Blas, G., Michaut, M., Treviño, C. L., Tomes, C. N., Yunes, R., Darszon, A., and Mayorga, L. S. (2002) The intraacrosomal calcium pool plays a direct role in acrosomal exocytosis. *J. Biol. Chem.* **277**, 49326–49331

48. Ménétrey, J., Macia, E., Pasqualato, S., Franco, M., and Cherfils, J. (2000) Structure of Arf6-GDP suggests a basis for guanine nucleotide exchange factors specificity. *Nat. Struct. Biol.* **7**, 466–469

49. Hu, T., Liu, Z., and Shen, X. (2011) Roles of phospholipase D in phorbol myristate acetate-stimulated neutrophil respiratory burst. *J. Cell Mol. Med.* **15**, 647–653

50. Scott, S. A., Selvy, P. E., Buck, J. R., Cho, H. P., Criswell, T. L., Thomas, A. L., Armstrong, M. D., Arteaga, C. L., Lindsley, C. W., and Brown, H. A. (2009) Design of isoform-selective phospholipase D inhibitors that modulate cancer cell invasiveness. *Nat. Chem. Biol.* **5**, 108–117

51. Horowitz, L. F., Hirdes, W., Suh, B. C., Hilgemann, D. W., Mackie, K., and Hille, B. (2005) Phospholipase C in living cells: activation, inhibition, Ca^{2+} requirement, and regulation of M current. *J. Gen. Physiol.* **126**, 243–262

52. Powis, G., and Phil, D. (1994) Inhibitors of phosphatidylinositol signalling as antiproliferative agents. *Cancer Metastasis Rev.* **13**, 91–103

53. Herrick, S. B., Schweissinger, D. L., Kim, S. W., Bayan, K. R., Mann, S., and Cardullo, R. A. (2005) The acrosomal vesicle of mouse sperm is a calcium store. *J. Cell. Physiol.* **202**, 663–671

54. Darszon, A., Nishigaki, T., Wood, C., Treviño, C. L., Felix, R., and Beltrán, C. (2005) Calcium channels and Ca^{2+} fluctuations in sperm physiology. *Int. Rev. Cytol.* **243**, 79–172

55. Suhaiman, L., De Blas, G. A., Obeid, L. M., Darszon, A., Mayorga, L. S., and Belmonte, S. A. (2010) Sphingosine 1-phosphate and sphingosine kinase are involved in a novel signaling pathway leading to acrosomal exocytosis. *J. Biol. Chem.* **285**, 16302–16314

56. Bello, O. D., Zanetti, M. N., Mayorga, L. S., and Michaut, M. A. (2012) RIM, Munc13, and Rab3A interplay in acrosomal exocytosis. *Exp. Cell Res.* **318**, 478–488

57. Coppola, T., Perret-Menoud, V., Gattesco, S., Magnin, S., Pombo, I., Blank, U., and Regazzi, R. (2002) The death domain of Rab3 guanine nucleotide exchange protein in GDP/GTP exchange activity in living cells. *Biochem. J.* **362**, 273–279

58. Cohen, L. A., Honda, A., Varnai, P., Brown, F. D., Balla, T., and Donaldson, J. G. (2007) Active Arf6 recruits ARNO/cytohesin GEFs to the PM by binding their PH domains. *Mol. Biol. Cell* **18**, 2244–2253

59. Santy, L. C., and Casanova, J. E. (2001) Activation of ARF6 by ARNO stimulates epithelial cell migration through downstream activation of both Rac1 and phospholipase D. *J. Cell Biol.* **154**, 599–610

60. Donaldson, J. G. (2005) Arfs, phosphoinositides and membrane traffic. *Biochem. Soc. Trans.* **33**, 1276–1278

61. Dong, N., Zhu, Y., Lu, Q., Hu, L., Zheng, Y., and Shao, F. (2012) Structurally distinct bacterial TBC-like GAPs link Arf GTPase to Rab1 inactivation to counteract host defenses. *Cell* **150**, 1029–1041

62. Arora, D. K., Syed, I., Machhadieh, B., McKenna, C. E., and Kowluru, A. (2012) Rab-geranylgeranyl transferase regulates glucose-stimulated insulin secretion from pancreatic β cells. *Islets* **4**, 354–358

63. Meyer, M. Z., Déliot, N., Chasserot-Golaz, S., Premont, R. T., Bader, M. F.,

and Vitale, N. (2006) Regulation of neuroendocrine exocytosis by the ARF6 GTPase-activating protein GIT1. *J. Biol. Chem.* **281,** 7919–7926

64. Di Paolo, G., Pellegrini, L., Letinic, K., Cestra, G., Zoncu, R., Voronov, S., Chang, S., Guo, J., Wenk, M. R., and De Camilli, P. (2002) Recruitment and regulation of phosphatidylinositol phosphate kinase type 1 γ by the FERM domain of talin. *Nature* **420,** 85–89

65. Funakoshi, Y., Hasegawa, H., and Kanaho, Y. (2011) Regulation of PIP5K activity by Arf6 and its physiological significance. *J. Cell. Physiol.* **226,** 888–895

66. Cockcroft, S. (2001) Signalling roles of mammalian phospholipase D1 and D2. *Cell. Mol. Life Sci.* **58,** 1674–1687

67. Dyer, N., Rebollo, E., Domínguez, P., Elkhatib, N., Chavrier, P., Daviet, L., González, C., and González-Gaitán, M. (2007) Spermatocyte cytokinesis requires rapid membrane addition mediated by ARF6 on central spindle recycling endosomes. *Development* **134,** 4437–4447

68. Baker, M. A., Hetherington, L., Reeves, G. M., and Aitken, R. J. (2008) The mouse sperm proteome characterized via IPG strip prefractionation and LC-MS/MS identification. *Proteomics.* **8,** 1720–1730

69. Rhee, S. G. (1991) Inositol phospholipids-specific phospholipase C: interaction of the γ1 isoform with tyrosine kinase. *Trends Biochem. Sci.* **16,** 297–301

70. Tomes, C. N., McMaster, C. R., and Saling, P. M. (1996) Activation of mouse sperm phosphatidylinositol-4,5 bisphosphate-phospholipase C by zona pellucida is modulated by tyrosine phosphorylation. *Mol. Reprod. Dev.* **43,** 196–204

71. Nomikos, M., Elgmati, K., Theodoridou, M., Georgilis, A., Gonzalez-Garcia, J. R., Nounesis, G., Swann, K., and Lai, F. A. (2011) Novel regulation of PLCζ activity via its XY-linker. *Biochem. J.* **438,** 427–432

72. Falkenburger, B. H., Dickson, E. J., and Hille, B. (2013) Quantitative properties and receptor reserve of the DAG and PKC branch of G(q)-coupled receptor signaling. *J. Gen. Physiol.* **141,** 537–555

73. Yoon, S. Y., Eum, J. H., Lee, J. E., Lee, H. C., Kim, Y. S., Han, J. E., Won, H. J., Park, S. H., Shim, S. H., Lee, W. S., Fissore, R. A., Lee, D. R., and Yoon, T. K. (2012) Recombinant human phospholipase C ζ1 induces intracellular calcium oscillations and oocyte activation in mouse and human oocytes. *Hum. Reprod.* **27,** 1768–1780

74. Nomikos, M., Blayney, L. M., Larman, M. G., Campbell, K., Rossbach, A., Saunders, C. M., Swann, K., and Lai, F. A. (2005) Role of phospholipase C-ζ domains in Ca²⁺-dependent phosphatidylinositol 4,5-bisphosphate hydrolysis and cytoplasmic Ca²⁺ oscillations. *J. Biol. Chem.* **280,** 31011–31018

75. Smrcka, A. V., Brown, J. H., and Holz, G. G. (2012) Role of phospholipase Cε in physiological phosphoinositide signaling networks. *Cell. Signal.* **24,** 1333–1343

76. Oestreich, E. A., Wang, H., Malik, S., Kaproth-Joslin, K. A., Blaxall, B. C., Kelley, G. G., Dirksen, R. T., and Smrcka, A. V. (2007) Epac-mediated activation of phospholipase Cε plays a critical role in β-adrenergic receptor-dependent enhancement of Ca²⁺ mobilization in cardiac myocytes. *J. Biol. Chem.* **282,** 5488–5495

77. Ebinu, J. O., Bottorff, D. A., Chan, E. Y., Stang, S. L., Dunn, R. J., and Stone, J. C. (1998) RasGRP, a Ras guanyl nucleotide-releasing protein with calcium- and diacylglycerol-binding motifs. *Science* **280,** 1082–1086

78. Mayorga, L. S., Tomes, C. N., and Belmonte, S. A. (2007) Acrosomal exo-cytosis, a special type of regulated secretion. *IUBMB Life* **59,** 286–292

79. Guo, X., Shen, J., Xia, Z., Zhang, R., Zhang, P., Zhao, C., Xing, J., Chen, L., Chen, W., Lin, M., Huo, R., Su, B., Zhou, Z., and Sha, J. (2010) Proteomic analysis of proteins involved in spermiogenesis in mouse. *J. Proteome Res.* **9,** 1246–1256

80. Wang, G., Guo, Y., Zhou, T., Shi, X., Yu, J., Yang, Y., Wu, Y., Wang, J., Liu, M., Chen, X., Tu, W., Zeng, Y., Jiang, M., Li, S., Zhang, P., *et al.* (2013) In-depth proteomic analysis of the human sperm reveals complex protein compositions. *J. Proteomics* **79,** 114–122

81. Mizuno-Yamasaki, E., Rivera-Molina, F., and Novick, P. (2012) GTPase networks in membrane traffic. *Annu. Rev. Biochem.* **81,** 637–659

82. Casanova, J. E. (2007) Regulation of Arf activation: the Sec7 family of guanine nucleotide exchange factors. *Traffic* **8,** 1476–1485

83. Sakagami, H. (2008) The EFA6 family: guanine nucleotide exchange factors for ADP ribosylation factor 6 at neuronal synapses. *Tohoku J. Exp. Med.* **214,** 191–198

84. Sakurai, A., Jian, X., Lee, C. J., Manavski, Y., Chavakis, E., Donaldson, J., Randazzo, P. A., and Gutkind, J. S. (2011) Phosphatidylinositol-4-phosphate 5-kinase and GEP100/Brag2 protein mediate antiangiogenic signaling by semaphorin 3E-plexin-D1 through Arf6 protein. *J. Biol. Chem.* **286,** 34335–34345

85. Macia, E., Partisani, M., Favard, C., Mortier, E., Zimmermann, P., Carlier, M. F., Gounon, P., Luton, F., and Franco, M. (2008) The pleckstrin homology domain of the Arf6-specific exchange factor EFA6 localizes to the plasma membrane by interacting with phosphatidylinositol 4,5-bisphosphate and F-actin. *J. Biol. Chem.* **283,** 19836–19844

86. Suzuki, R., Saino-Saito, S., Sakagami, H., Toshimori, K., Abe, H., and Kondo, H. (2009) Localization of EFA6A, a guanine nucleotide exchange factor for ARF6, in spermatogenic cells of testes of adult mice. *J. Mol. Histol.* **40,** 77–80

87. Baker, M. A., Naumovski, N., Hetherington, L., Weinberg, A., Velkov, T., and Aitken, R. J. (2013) Head and flagella subcompartmental proteomic analysis of human spermatozoa. *Proteomics* **13,** 61–74

88. Fukaya, M., Fukushima, D., Hara, Y., and Sakagami, H. (2014) EFA6A, a guanine nucleotide exchange factor for Arf6, interacts with sorting nexin-1 and regulates neurite outgrowth. *J. Neurochem.* **129,** 21–36

89. Scholz, R., Berberich, S., Rathgeber, L., Kolleker, A., Köhr, G., and Kornau, H. C. (2010) AMPA receptor signaling through BRAG2 and Arf6 critical for long-term synaptic depression. *Neuron* **66,** 768–780

90. Zanetti, S. R., Monclus Mde L., Rensetti, D. E., Fornés, M. W., and Aveldaño, M. I. (2010) Differential involvement of rat sperm choline glycerophospholipids and sphingomyelin in capacitation and the acrosomal reaction. *Biochimie* **92,** 1886–1894

91. Zanetti, S. R., de Los Ángeles Monclus, M., Rensetti, D. E., Fornés, M. W., and Aveldaño, M. I. (2010) Ceramides with 2-hydroxylated, very long-chain polyenoic fatty acids in rodents: From testis to fertilization-competent spermatozoa. *Biochimie* **92,** 1778–1786

92. Jungnickel, M. K., Sutton, K. A., Wang, Y., and Florman, H. M. (2007) Phosphoinositide-dependent pathways in mouse sperm are regulated by egg ZP3 and drive the acrosome reaction. *Dev. Biol.* **304,** 116–126

93. Bohring, C., and Krause, W. (1999) The characterization of human spermatozoa membrane proteins–surface antigens and immunological infertility. *Electrophoresis* **20,** 971–976